

Research Article

“In Silico” Characterization of 3-Phytase A and 3-Phytase B from *Aspergillus niger*

Doris C. Niño-Gómez,¹ Claudia M. Rivera-Hoyos,¹ Edwin D. Morales-Álvarez,² Edgar A. Reyes-Montaño,³ Nury E. Vargas-Alejo,³ Ingrid N. Ramírez-Casallas,¹ Kübra Erkan Türkmen,⁴ Homero Sáenz-Suárez,⁵ José A. Sáenz-Moreno,⁵ Raúl A. Poutou-Piñales,¹ Janneth González-Santos,⁶ and Azucena Arévalo-Galvis⁷

¹Laboratorio de Biotecnología Molecular, Grupo de Biotecnología Ambiental e Industrial (GBAI), Departamento de Microbiología, Facultad de Ciencias, Pontificia Universidad Javeriana, Bogotá, Colombia

²Departamento de Química, Facultad de Ciencias Exactas y Naturales, Universidad de Caldas, Manizales, Caldas, Colombia

³Grupo de Investigación en Proteínas, Departamento de Química, Facultad de Ciencias, Universidad Nacional de Colombia (UNAL), Bogotá, Colombia

⁴Department of Biology, Faculty of Science, Hacettepe University, Beytepe, Ankara, Turkey

⁵Unidad de Biología Celular y Microscopía, Decanato de Ciencias de la Salud, Universidad Centroccidental Lisandro Alvarado, Barquisimeto, Venezuela

⁶Grupo de Bioquímica Computacional y Estructural, Departamento de Bioquímica y Nutrición, Facultad de Ciencias, Pontificia Universidad Javeriana, Bogotá, Colombia

⁷Laboratorio de Microbiología Especial, Grupo de Enfermedades Infecciosas, Departamento de Microbiología, Facultad de Ciencias, Pontificia Universidad Javeriana, Bogotá, Colombia

Correspondence should be addressed to Edgar A. Reyes-Montaño; eareyesm@unal.edu.co and Raúl A. Poutou-Piñales; rpoutou@javeriana.edu.co

Received 31 May 2017; Accepted 27 July 2017; Published 20 November 2017

Academic Editor: Sunney I. Chan

Copyright © 2017 Doris C. Niño-Gómez et al. This is an open access article distributed under the Creative Commons Attribution License, which permits unrestricted use, distribution, and reproduction in any medium, provided the original work is properly cited.

Phytases are used for feeding monogastric animals, because they hydrolyze phytic acid generating inorganic phosphate. *Aspergillus niger* 3-phytase A (PDB: 3K4Q) and 3-phytase B (PDB: 1QFX) were characterized using bioinformatic tools. Results showed that both enzymes have highly conserved catalytic pockets, supporting their classification as histidine acid phosphatases. 2D structures consist of 43% alpha-helix, 12% beta-sheet, and 45% others and 38% alpha-helix, 12% beta-sheet, and 50% others, respectively, and pI 4.94 and 4.60, aliphatic index 72.25 and 70.26 and average hydrophobicity of -0.304 and -0.330 , respectively, suggesting aqueous media interaction. Glycosylation and glycation sites allowed detecting zones that can affect folding and biological activity, suggesting fragmentation. Docking showed that H₅₉ and H₆₃ act as nucleophiles and that D₃₃₉ and D₃₁₉ are proton donor residues. MW of 3K4Q (48.84 kDa) and 1QFX (50.78 kDa) is similar; 1QFX forms homodimers which will originate homotetramers with several catalytic center accessible to the ligand. 3K4Q is less stable (instability index 45.41) than 1QFX (instability index 33.66), but the estimated lifespan for 3K4Q is superior. Van der Waals interactions generate hydrogen bonds between the active center and O₂ or H of the phytic acid phosphate groups, providing greater stability to these temporal molecular interactions.

1. Introduction

Most of the phosphorus (P) present in terrestrial ecosystems is located in the soil. Globally, the terrestrial biota contains

2.6×10^6 g P, which is less than that contained in the soil, which oscillates between 96 and 160×10^6 g P [1]. The highest transference of P from soil to biota occurs through the synthesis of organic compounds containing phosphorus (P)

in plants, animals, and microorganisms. The organic compounds containing P are diverse, and their mineralization in the soil allows the P to be recycled back to the biota [1].

Phosphorus is an essential nutrient, which is involved in several biological functions such as regulation of intra- and extracellular pH, accumulation of energy in the form of ATP, lipid transport, and formation of biological membranes [2, 3]. Several compounds with organic phosphorus (oP) have different rates of mineralization. For example, oP from microorganisms (predominantly nucleic acids, 30–50% P in RNA and 5–10% P in DNA) and phospholipids (<10% P) is easily mineralized in soil environments [1]. However, other compounds with oP are not easily mineralized and can accumulate in the soil in substantial amounts. The most significant of these compounds is phytic acid (myo-inositol 1, 2, 3, 4, 5, 6 hexakisphosphate), [1].

Phytic acid is the main form of P storage in cereals, pulses, oilseeds, and nuts and constitutes 1–5% of its dry weight. In forage, one-third of the phosphorus is present as digestible inorganic phosphorus (iP), while the remaining two-thirds are present as oP in the form of phytates [4]. Phytates are a mixture of salts resulting from the union of phytic acid with divalent metal ions such as: Calcium (Ca^{2+}), Copper (Cu^{2+}), Iron (Fe^{2+}), Magnesium (Mg^{2+}), Manganese (Mn^{2+}), and Zinc (Zn^{2+}). Phytic acid can be bound to two different metals such as Calcium (Ca^{2+}) and Magnesium (Mg^{2+}), the resulting mixed salt is called phytin [4].

Phytate constitutes 65–80% of total P in grains and up to 80% of total P in manures of monogastric animals. Due to its negative charge, phytate is strongly adsorbed to various soil components once it is released from plant residues or manure [1].

On the other hand, the accumulation of phytate in the soil is due to the low possibility of being hydrolyzed by the phytase enzymes (E.C. 3.1.3.8), since the phytate dephosphorylation requires the binding of free phytate to the binding pocket of the substrate in the phytase enzyme. Thus, if phytate is tightly bound with soil components, it is not susceptible to be hydrolyzed by enzymes [1].

P from phytate is largely unavailable for monogastric animals, such as pigs and birds, due to the absence or the insufficient amount of phytase enzymes in the gastrointestinal tract to degrade it [5]; in this way it passes without being digested through the gastrointestinal tract. Since phytic acid can not be reabsorbed, feed for pigs and poultry is commonly supplemented with iP in order to meet the requirement of P, which increases production costs [6].

Supplementation with iP, along with the P from phytate excreted by monogastric animals, generates global ecological problems (eutrophication) as the discharge into rivers of wastewater with a high content of phytates results in the proliferation of cyanobacteria, hypoxia, and death of animals from aquatic environments [5]. The P present in phytate that is excreted in the manure of monogastric animals subsequently extends to farmlands, which often contributes to the eutrophication of surface waters, particularly in the areas of intensive livestock of pigs [7].

However, the adverse environmental and nutritional consequences of the presence of phytate in the diet of monogastric animals can be improved by the inclusion of phytases (E.C. 3.1.3.8) in their diet [5]. These enzymes are considered as an environmentally friendly product because (i) they reduce the amount of phosphorus entering the ecosystem, (ii) they reduce the problems caused by eutrophication of water, and (iii) they reduce the constant chelation or sequestration of nutritional factors in the soil, as well as in the digestive tract of poultry and pigs [8]. Phytases are produced by a wide variety of plants, bacteria, fungi, and yeasts. A commercial pair of phytases from the genus *Aspergillus* (Natuphos® and Ronozyme®) are currently available, as these filamentous fungi are the most prolific extracellular producers of this enzyme [7].

Some studies have shown that microbial sources are more promising for commercial phytase production. Although several strains of bacteria, yeasts, and fungi have been used for production under different conditions, two species, *A. niger* and *A. ficuum*, have been used more frequently for commercial phytase production [9]. Among the best known commercial phytases is found “Natu-phos” (Gist-Brocades NV Company, Netherlands). Natu-phos is a recombinant phytase produced by the expression of the *phyA* gene of *A. ficuum* NRRL 3135 in *A. niger* CBS 513.88, produced in 1994 [4, 7, 9].

In countries like Colombia and Venezuela, there is no legislation regulating the incorporation of phytase enzymes into the feed of monogastric animals, aimed at improving the bioavailability of phosphorus from the diet itself and at the reduction of the amount of phytate excreted in the feces. Therefore, the “in silico” analysis of physicochemical and structural properties, as well as the molecular docking analysis between the enzymes and the ligand, will allow researchers to gather information that is useful for the heterologous expression of the recombinant enzymes.

2. Materials and Methods

2.1. Protein Analysis. The phytases reported until September 13, 2015, were analyzed in the UNIPROT database (The UniProt Consortium) [10]. The PSI-Blast alignment [11] was performed between the amino acid sequences of the phytase reported for *A. niger*, which allowed determining its percentage of similarity and a multiple alignment with the ClustalO programs to identify conserved sites among the selected phytases. The ClustalW alignment allowed comparing the sequences of the two revised phytases: the 3-phytase A and the chains A and B of the 3-phytase B (<http://www.ebi.ac.uk>) [12].

2.2. Bioinformatic Analysis of the Reported and Revised Phytase from *A. Niger*. For this analysis, two protein structures resolved by X-ray crystallography (revised proteins) were used for *A. niger*: 3-phytase A and 3-phytase B. The primary sequences of the revised phytases were obtained from UniProtKB, Entry: P34755 and P34752, respectively, while tertiary structures were obtained from Protein Data Bank (PDB) [13], using the ID: 3K4Q and 1QFX, respectively.

2.3. Physicochemical Properties. The physicochemical properties of the amino acid sequences of the revised *A. niger* proteins were evaluated using the following programs: ProtParam and ProtScale [14] from ExPASy (<http://www.expasy.org>). The size of the window for the analyses with ProtScale was the basic nine amino acids recommended by the programs to ensure optimum coverage of the sequence when the path is made over it. In the case of the hydrophobicity profile, the Kyte and Doolittle algorithm was used, whose scale considers values between -4.5 and 4.5 . The 3D structures of phytases from *A. niger* were visualized using the PyMOL (The PyMOL Molecular Graphics System, Version 1.8 Schrödinger, LLC) program.

2.4. Prediction of N-Glycosylation Sites. For the analysis of potential N-glycosylation sites in both phytases, the NetNGlyc 1.0 software [15] (<http://www.cbs.dtu.dk>) was used.

2.5. Prediction of Glycation Sites. For the analysis of the potential glycation sites in both phytases, Netglycate 1.0 software was used [16]. In addition, visualization of the 3D structures and determination of the distances between the ϵ -NH₂ groups of the lysines and the side chains of Glutamate acid residues (E) and Aspartate (D) or basic residues of histidine (H), Arginine (R), and lysine (K) were performed using the SPDB-viewer 4.01 program [17, 18].

2.6. Prediction of Antigenic Peptides. Prediction of antigenic peptides in both proteins was performed by means of the antigenic peptide prediction tool (<http://imed.med.ucm.es/Tools/antigenic.pl>) [19] of the Complutense University of Madrid.

2.7. Ligand and Molecular Coupling Models (Rigid Docking). The construction of the ligand (phytic acid) was performed using the Spartan version 4.0 molecular modeling program (<https://www.wavefun.com/products/spartan.html>), which has a graphical interface that allows the construction of the molecule atom by atom, selecting the appropriate hybridization according to the binding site of each element, followed by a minimization of the energy of the generated model.

The molecular coupling models of the reviewed phytases from *A. niger* against the phytic acid as a ligand were performed using the Autodock program [20] and the 3D structure of the ligand (phytic acid) was obtained with the Spartan program (before performing simulations of coupling with Autodock 4.2) [20]. The pocket containing the amino acids that form the highly conserved catalytic center in the revised phytase (histidine acid phosphatases) from *A. niger* (RHGXRX-P-D) was identified from reports in the literature [21, 22]. Polar hydrogens were added to each receptor; the grid was located in the pocket of the active site for each model. Phytic acid boxes had the following dimensions and coordinates respectively: for 3-phytase A: X36, Y36 and Z38 ($x: -6.396$, $y: 8.301$ and $z: 27.885$), and for 3-phytase B: X36, Y34 and Z38 ($x: 23.968$, $y: 71.06$ and $z: 69.576$), with a space in both proteins of 0.375 Å. The network parameters and atomic affinity maps were calculated using AutoGrid 4 [20]. Each

coupling simulation was carried out using the Lamarckian genetic algorithm with 2.500.000 energetic evaluations with a population of 150. Finally, the best poses of the ligand were determined based on the results of energy interaction given in kcal/mol.

3. Results

3.1. Computational Characterization. Until September 13, 2015, there were 12651 phytases in UNIPROT of which 115 (0.90%) belonged to *Aspergillus* spp., of which, 33 (28.69%) belonged to *A. niger*. For the genus *Aspergillus*, 11 phytases in total were reported as revised or cured; the distribution was as follows: one for each species *A. ficuum*, *A. oryzae*, *A. fumigatus*, and *A. nidulans*; two for *A. niger* and *A. awamori*, and three for *A. terreus*. The only two (6.06%) of the revised phytases of *A. niger* were 3-phytase A (E.C. 3.1.3.8, PDB ID: 3K4Q), corresponding to a monomer, and the 3-phytase B (E.C. 3.1.3.8, PDB ID: 1QFX), a homodimer.

The dendrogram between the 33 phytases reported for *A. niger* was obtained using the BLAST tool, and it was found that 3-phytase A (number 17, P34752) is closely related to 78.8% (26/33) of phytases whereas 3-phytase B (number 5, P34754) is only related to 9.1% (3/33) (Figure 1).

The multiple alignment (Clustal O) between the amino acid sequences of the phytases reported for *A. niger* enabled the identification of a highly conserved sequence (RHGXRX-P-HD) present in the histidine acid phosphatase family, corresponding to the pocket where the active ligand binding site is located (Figure 2).

3.2. Structural Characteristics of the Two Reported and Revised Phytases from A. Niger. The first revised phytase from *A. niger*, the 3-phytase A (PDB ID: 3K4Q), corresponds to a monomer. The second revised phytase, the 3-phytase B (PDB ID: 1QFX), initially corresponds to a homodimer (Chains A and B) which, thanks to its crystallographic symmetry, generates a homotetramer from two dimers.

When performing an alignment (Clustal W) between the sequences of the two chains of the initially dimeric protein (A and B) and the unique sequence of the monomeric protein, it was possible to determine that the chains A and B of the dimer are identical to each other, but different to the monomeric phytase.

3.3. 2D Structures of the Two Reported and Revised Phytases from A. Niger. The 3-phytase A (monomer) (Figure 3) (PDB ID: 3K4Q) has a 2D structure formed by 43% alpha helices, 12% beta sheets, and 45% random coils. A and B chains of 3-phytase B initially form a homodimer (Figure 3) (PDB ID: 1QFX) and its 2D structure corresponds to 38% alpha helices, 12% beta sheets, and 50% random coils. For the 3-phytase A, the active site is conformed by amino acids R₅₈, H₅₉, R₆₂, R₁₄₂, and D₃₃₉ [22] (Figure 3(b)), and for the 3-phytase B the active site is conformed by amino acids R₆₂, H₆₃, R₆₆, R₁₅₆, H₃₁₈, and D₃₁₉ [21] (Figures 3(c) and 3(d)).

3.4. Structure of the Homodimer and the Tetramer Formed by Chains A and B of the 3-Phytase B from A. Niger. 3-phytase

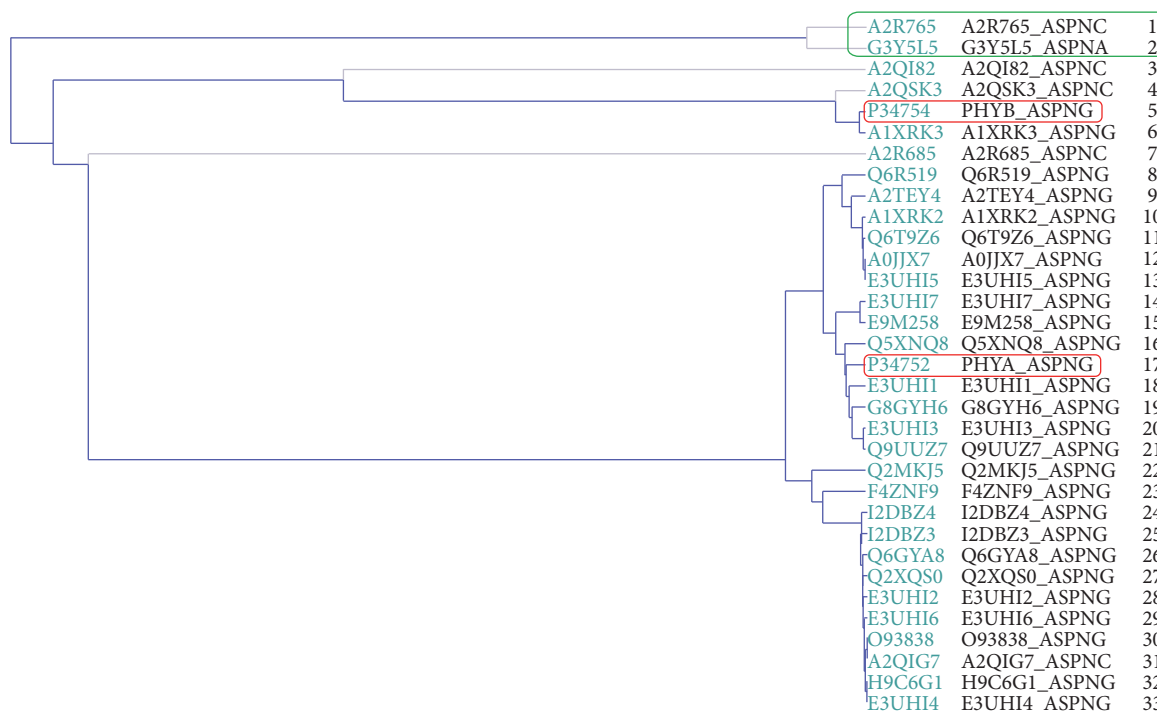


FIGURE 1: Dendrogram of the 33 phytases reported for *A. niger*. The first two phytases that appear are phytases that do not have PDB code or are not characterized within UNIPROT and are far from the two revised phytases. Alignment parameters are predetermined. The default transition matrix is Gonnet; the gap of the opening is 6 bits; the extension interval is of 1 bit. Clustal-Omega uses the HHafign algorithm and its default configuration as its core alignment engine [23].

B is initially a homodimer consisting of two identical chains A and B. The 39 amino acids that allow the interactions that lead to dimerization between the A and B chains are: Lys₁₄-Tyr₂₄, Leu₂₇-His₂₉, Tyr₃₆, Glu₃₈, Ser₄₁-Ala₄₅, Tyr₁₂₀, Lys₂₁₇, Leu₂₄₈, Pro₂₅₂-Ser₂₅₄, Gln₂₆₂-Asp₂₆₃, Val₂₆₆-Ser₂₆₇, Asn₃₃₅, Arg₃₄₂, Phe₃₄₅-Gly₃₄₆, Ala₃₇₂, Asp₃₉₃, Gly₃₉₉, Tyr₄₀₀. The crystallographic symmetry generates a tetramer from the two dimers, and 17 amino acids that are involved in the interactions that allow the tetramerization of the protein have been identified: Cys₁₀₉, Glu₁₁₄, Thr₁₁₆, Gly₁₁₈, Ala₁₂₁, Leu₁₂₃-Leu₁₂₄, Tyr₁₂₇-Asn₁₂₈, Asn₁₃₁, Lys₁₆₃, Glu₁₆₆, Tyr₁₇₁, Arg₄₄₇, Pro₄₅₀-Ile₄₅₁, and Cys₄₅₃ [21] (Figures 3(e) and 3(f)).

In both phytases, the fact that the pocket of the active site is composed mostly of positively charged amino acids (Histidine and R-Arginine) is highlighted.

3.5. Physicochemical Characterization of the Two Reported and Revised Phytases from *A. Niger*. The physicochemical properties of the two phytases reported and reviewed for *A. niger* and obtained by the ProtParam bioinformatics program are detailed in Table 1.

3.6. Hydrophobicity and Accessibility Profiles of the Two Reported and Revised Phytases from *A. niger*. Figures 4(a) and 4(b) are the detailed hydrophobicity profiles of the phytases A and B from *A. niger*. The red circles represent the amino acids with a higher hydrophobicity score and the yellow circles represent the amino acids with a lower

hydrophobicity score, according to the values recorded in Table 2.

The accessibility profile of phytases A and B from *A. niger* is shown in Figure 5. Green colored circles represent amino acids with a minimum accessibility value and purple circles represent amino acids with a maximum accessibility value, according to the values recorded in Table 2.

3.7. Prediction of N-Glycosylation Sites in 3-Phytase A and Chain A of 3-Phytase B from *A. Niger*. Table 3 details the predictions of possible N-glycosylation sites of phytases A and B from *A. niger* by means of the NetNGlyc 1.0 tool, showing the position of the Asparagines (N), along both phytase chains that are located in an Asn-Xaa-Ser/Thr (where Xaa is any amino acid except proline) and for that reason could be glycosylated.

3.8. Prediction of Glycation Sites in 3-Phytase A and Chain A of 3-Phytase B from *A. Niger*. In the case of 3-phytase A, Netglycate 1.0 predicted the glycation potential of seven lysines, whereas the methodology proposed by Sáenz et al., 2016 suggests the glycation of 14 of them. For Lys94, there is no prediction of glycation by either method. Table 4 shows the comparison of the results and distances of the ϵ -NH₂ groups of the lysines and the side chains of acidic or basic residues. Figure 6 shows some distances between lysines and other acidic or basic residues in 3-phytase A.

In the case of 3-phytase A, Netglycate 1.0 allowed predicting the glycation potential of seven lysines along the protein

1	P34752	PHYA_ASPNG	63	-----ISPEVPAGCRVTF	RAQLVSRHGR	YPTDSK	GKKYSALIEEIQ	---QNATTFDGKY	113	
2	P34754	PHYB_ASPNG	63	-----IARDPPTGCEVDQVIMV	KRHGER	YSPSAGK	SIEEALAKVYSI	-NTT-EYK	GDL 114	
3	A2QSK3	A2QSK3_ASPNC	63	-----IARDPPTGCEVDQVIMV	KRHGER	YSPSAGK	SIEEALAKVYSI	-NTT-EYK	GDL 114	
4	A2QIG7	A2QIG7_ASPNC	63	-----ISPDVPA	GCHVTF	RAQLVSRHGR	YPTDSK	GKKYSALIEEIQ	---QNATTFEGKY 113	
5	H9C6G1	H9C6G1_ASPNG	63	-----ISPDVPA	GCHVTF	RAQLVSRHGR	YPTDSK	GKKYSALIEEIQ	---QNATTFEGKY 113	
6	A1XRK3	A1XRK3_ASPNG	47	-----IARDPPTGCEVDQVIMV	KRHGER	YSPSAGK	SIEEALAKVYSI	-NTT-EYK	GDL 98	
7	I2DBZ3	I2DBZ3_ASPNG	63	-----ISPDVPA	GCHVTF	RAQLVSRHGR	YPTDSK	GKKYSALIEEIQ	---QNATTFEGKY 113	
8	I2DBZ4	I2DBZ4_ASPNG	63	-----ISPDVPA	GCHVTF	RAQLVSRHGR	YPTDSK	GKKYSALIEEIQ	---QNATTFEGKY 113	
9	G8GYH6	G8GYH6_ASPNG	63	-----ISPDVPA	GKVTFA	RAQLVSRHGR	YPTDSK	GKKYSALIEEIQ	---QNATTFDGKY 113	
11	A1XRK2	A1XRK2_ASPNG	44	-----ISPEVPAGCRVTF	RAQLVSRHGR	YPTDSK	GKKYSALIEEIQ	---QNATTFDGKY 94		
12	A0JX7	A0JX7_ASPNG	48	-----ISPEVPAGCRVTF	RAQLVSRHGR	YPTDSK	GKKYSALIEEIQ	---QNATTFDGKY 98		
13	Q2XQSO	Q2XQSO_ASPNG	44	-----ISPDVPA	GCHVTF	RAQLVSRHGR	YPTDSK	GKKYSALIEEIQ	---QNATTFEGKY 94	
14	Q6GYA8	Q6GYA8_ASPNG	44	-----ISPDVPA	GCHVTF	RAQLVSRHGR	YPTDSK	GKKYSALIEEIQ	---QNATTFEGKY 94	
15	Q9UUZ7	Q9UUZ7_ASPNG	63	-----ISPDVPA	GCRVTF	RAQLVSRHGR	YPTDSK	GKKYSALIEEIQ	---QNATTFDGKY 113	
16	O93838	O93838_ASPNG	63	-----ISPDVPA	GCHVTF	RAQLVSRHGR	YPTDSK	GKKYSALIEEIQ	---QNATTFEGKY 113	
17	Q6T9Z6	Q6T9Z6_ASPNG	63	-----ISPEVPAGCRVTF	RAQLVSRHGR	YPTDSK	GKKYSALIEEIQ	---QNATTFDGKY 113		
18	Q6R519	Q6R519_ASPNG	63	-----ISPDVPA	GCRVTF	RAQLVSRHGR	YPTDSK	GKKYSALIEEIQ	---QNATTFDGKY 113	
19	A2TEY4	A2TEY4_ASPNG	63	-----ISPEVPAGCRVTF	RAQLVSRHGR	YPTDSK	GKKYSALIEEIQ	---QNATTFDGKY 113		
20	Q5XNQ8	Q5XNQ8_ASPNG	63	-----ISPDVPA	GKVTFA	RAQLVSRHGR	YPTDSK	GKKYSALIEEIQ	---QNATTFDGKY 113	
22	F4ZNF9	F4ZNF9_ASPNG	90	-----ISPDVPA	GQVTF	RAQLVSRHGR	YPTDSK	GKKYSALIEEIQ	---QNATTFEKY 140	
23	A2QI82	A2QI82_ASPNC	59	-----ISRDPPA	QCSVDQVIMV	KRHGER	YPTGEGTSIEQTLK	INDS-LAGN	YSSGDL 111	
24	A2R685	A2R685_ASPNC	111	-----DEFPRP	GSNITQMHML	HRHGR	SRYPNK	DEGDDFANWIK	AITNATAHGA	VFRDEL 164
25	E3UH11	E3UH11_ASPNG	44	-----ISPDVPA	GCRVTF	RAQLVSRHGR	YPTDSK	GKKYSALIEEIQ	---QNATTFDGKY 94	
26	E3UH14	E3UH14_ASPNG	44	-----ISPDVPA	GCHVTF	RAQLVSRHGR	YPTDSK	GKKYSALIEEIQ	---QNATTFEGKY 94	
27	E3UH13	E3UH13_ASPNG	44	-----ISPDVPA	GCRVTF	RAQLVSRHGR	YPTDSK	GKKYSALIEEIQ	---QNATTFDGKY 94	
28	E3UH12	E3UH12_ASPNG	44	-----ISPDVPA	GCHVTF	RAQLVSRHGR	YPTDSK	GKKYSALIEEIQ	---QNATTFEGKY 94	
29	E3UH16	E3UH16_ASPNG	44	-----ISPDVPA	GCHVTF	RAQLVSRHGR	YPTDSK	GKKYSALIEEIQ	---QNATTFEGKY 94	
30	E3UH15	E3UH15_ASPNG	44	-----ISPEVPAGCRVTF	RAQLVSRHGR	YPTDSK	GKKYSALIEEIQ	---QNATTFDGKY 94		
31	E9M258	E9M258_ASPNG	44	-----ISPDVPA	GCRVTF	RAQLVSRHGR	YPTESK	GKKYSALIEEIQ	---QNVTFDGKY 94	
32	Q2MKJ5	Q2MKJ5_ASPNG	47	-----ISPDVPA	GCHVTF	RAQLVSRHGR	YPTDSK	GKKYSALIEEIQ	---QNATTFEGKY 97	
33	E3UH17	E3UH17_ASPNG	44	-----ISPDVPA	GCRVTF	RAQLVSRHGR	YPTESK	GKKYSALIEEIQ	---QNVTFDGKY 94	
	A2R765	A2R765_ASPNC	117	LSPNASATH	SPSPNHL	HYLDTLL	LTGPDN	-----APLTGLDAITTTT	TTTT-TTKY 168	
	G3Y5L5	G3Y5L5_ASPNA	109	LSPNASATH	SPSPNHL	HYLDTLL	LTGPDN	-----APLTGLDAITTTT	TTTT-TTKY 160	

1	P34752	PHYA_ASPNG	114	AFLK	TYNYS	LGADDLT	-----PFG	--EQELVNSG	IKFY	-QRYES	LRNI	----VPFI 158			
2	P34754	PHYB_ASPNG	115	AFLNDW	TYVYP	NECYNA	EAETTS	SGPYAG	--LLDAYN	HGNDYK	-ARYGH	LWNGET	---VVPF 168		
3	A2QSK3	A2QSK3_ASPNC	115	AFLNDW	TYVYP	NECYNA	EAETTS	SGPYAG	--LLDAYN	HGNEYK	-ARYGH	LWNGET	---VVPF 168		
4	A2QIG7	A2QIG7_ASPNC	114	AFLK	TYNYS	LGADDLT	-----PFG	--EQELVNSG	VKIFY	-QRYES	LRNI	----VPFI 158			
5	H9C6G1	H9C6G1_ASPNG	114	AFLK	TYNYS	LGADDLT	-----PFG	--EQELVNSG	VKIFY	-QRYES	LRNI	----VPFI 158			
6	A1XRK3	A1XRK3_ASPNG	99	AFLNDW	TYVYP	NECYNA	EAETTS	SGPYAG	--LLDAYN	HGNDYK	-ARYGH	LWNGET	---VVPF 152		
7	I2DBZ3	I2DBZ3_ASPNG	114	AFLK	TYNYS	LGADDLT	-----PFG	--EQELVNSG	VKIFY	-QRYES	LRNI	----VPFI 158			
8	I2DBZ4	I2DBZ4_ASPNG	114	AFLK	TYNYS	LGADDLT	-----PFG	--EQELVNSG	VKIFY	-QRYES	LRNI	----VPFI 158			
9	G8GYH6	G8GYH6_ASPNG	114	AFLK	TYNYS	LGADDLT	-----PFG	--EQELVNSG	IKFY	-QRYES	LRNI	----IPFI 158			
10	A1XRK2	A1XRK2_ASPNG	95	AFLK	TYNYS	LGADDLT	-----PFG	--EQELVNSG	IKLY	-QRYES	LRNI	----IPFI 139			
11	A0JX7	A0JX7_ASPNG	99	AFLK	TYNYS	LGADDLT	-----PFG	--EQELVNSG	IKFY	-QRYES	LRNI	----IPFI 143			
12	Q2XQSO	Q2XQSO_ASPNG	95	AFLK	TYNYS	LGADDLT	-----PFG	--EQELVNSG	VKIFY	-QRYES	LRNI	----VPFI 139			
13	Q6GYA8	Q6GYA8_ASPNG	95	AFLK	TYNYS	LGADDLT	-----PFG	--EQELVNSG	VKIFY	-QRYES	LRNI	----VPFI 139			
14	Q9UUZ7	Q9UUZ7_ASPNG	114	AFLK	TYNYS	LGADDLT	-----PFG	--EQELVNSG	IKFY	-QRYES	LRNI	----IPFI 158			
15	O93838	O93838_ASPNG	114	AFLK	TYNYS	LGADDLT	-----PFG	--EQELVNSG	VKIFY	-QRYES	LRNI	----VPFI 158			
16	Q6T9Z6	Q6T9Z6_ASPNG	114	AFLK	TYNYS	LGADDLT	-----PFG	--EQELVNSG	IKFY	-QRYES	LRNI	----IPFI 158			
17	Q6R519	Q6R519_ASPNG	114	AFLK	TYNYS	LGDDLT	-----PLG	--EQELVNSG	IKFY	-QRYES	LRNI	----IPFI 158			
18	A2TEY4	A2TEY4_ASPNG	114	AFLK	TYNYS	LGDDLT	-----PLG	--EQELVNSG	IKFY	-QRYES	LRNI	----IPFI 158			
19	Q5XNQ8	Q5XNQ8_ASPNG	114	AFLK	TYNYS	LGADDLT	-----PFG	--EQELVNSG	IKFY	-QRYES	LRNI	----IPFI 158			
20	F4ZNF9	F4ZNF9_ASPNG	141	AFLK	TYNYS	RMGADDLT	-----PFG	--EQELVNSG	VKIFY	-QRYES	LRNI	----VPFI 185			
21	A2QI82	A2QI82_ASPNC	112	AFLGNW	TYFV	PSDCY	-EAET	STGPYAG	--LNDAYN	HGKAYR	-QRYGN	LYNESS	---ILPL 164		
22	A2R685	A2R685_ASPNC	165	SFIH	DW	TYSLG	ADMLT	-----TRG	--REDL	LES	GILNF	-YNYGH	LYTPGT	---KIVA 210	
23	E3UH11	E3UH11_ASPNG	95	AFLK	TYNYS	LGADDLT	-----PFG	--EQELVNSG	IKFY	-QRYES	LRNI	----IPFI 139			
24	E3UH14	E3UH14_ASPNG	95	AFLK	TYNYS	LGADDLT	-----PFG	--EQELVNSG	VKIFY	-QRYES	LRNI	----VPFI 139			
25	E3UH13	E3UH13_ASPNG	95	AFLK	TYNYS	LGADDLT	-----PFG	--EQELVNSG	IKFY	-QRYES	LRNI	----IPFI 139			
26	E3UH12	E3UH12_ASPNG	95	AFLK	TYNYS	LGADDLT	-----PFG	--EQELVNSG	VKIFY	-QRYES	LRNI	----VPFI 139			
27	E3UH16	E3UH16_ASPNG	95	AFLK	TYNYS	LGADDLT	-----PFG	--EQELVNSG	VKIFY	-QRYES	LRNI	----VPFI 139			
28	E3UH15	E3UH15_ASPNG	95	AFLK	TYNYS	LGADDLT	-----PFG	--EQELVNSG	IKFY	-QRYES	LRNI	----IPFI 139			
29	E9M258	E9M258_ASPNG	95	AFLK	TYNYS	LGADDLT	-----PFG	--EQELVNSG	IKSY	-QRYES	LRNI	----IPFI 139			
30	Q2MKJ5	Q2MKJ5_ASPNG	98	AFLK	TYNYS	LGADDLT	-----PFG	--EQELVNSG	VKIFY	-QRYES	LRNI	----VPFI 142			
31	E3UH17	E3UH17_ASPNG	95	AFLK	TYNYS	LGADDLT	-----PFG	--EQELVNSG	IKFY	-QRYES	LRNI	----IPFI 139			
32	A2R765	A2R765_ASPNC	169	PNFP	----	PLPIATY	-PGD	GFGGPGGGHR	IPLDA	EGLALPA	HPA	HPA	IWV	SDEYGP	YVYK 223
33	G3Y5L5	G3Y5L5_ASPNA	161	PNFP	----	PLPIATY	-PGD	GFGGPGGGHR	IPLDA	EGLALPA	HPA	HPA	IWV	SDEYGP	YVYK 215

FIGURE 2: Continued.

1	P34752	PHYA_ASPNG	354	TLYADFSHDNGIISILFALGLYNGTK-PLSTTTVE-----NITQT-----	392
2	P34754	PHYB_ASPNG	330	PLFFNFAHDTNITPILAALGVLIPNE-DLPLDR-----VAFG-----	365
3	A2QSK3	A2QSK3_ASPNC	330	SLFFNFAHDTNITPILAALGVLIPTE-DLPLDR-----VAFG-----	365
4	A2QIG7	A2QIG7_ASPNC	354	TLYADFSHDNGIISILFALGLYNGTK-PLSSTTAE-----NITQT-----	392
5	H9C6G1	H9C6G1_ASPNG	354	TLYADFSHDNGIISILFALGLYNGTK-PLSSTTAE-----NITQT-----	392
6	A1XRK3	A1XRK3_ASPNG	314	PLFFNFAHDTNITPILAALGVLIPNE-DLPLDR-----VAFG-----	349
7	I2DBZ3	I2DBZ3_ASPNG	354	TLYADFSHDNGIISILFALGLYNGTK-PLSSTTAE-----NITQT-----	392
8	I2DBZ4	I2DBZ4_ASPNG	354	TLYADFSHDNGIISILFALGLYNGTK-PLSSTTAE-----NITQT-----	392
9	G8GYH6	G8GYH6_ASPNG	354	TLYADFSHDNGIISILFALGLYNGTK-PLSSTTAE-----NITQT-----	392
10	A1XRK2	A1XRK2_ASPNG	335	TLYADFSHDNGIISILFALGLYNGTK-PLSTTTVE-----NITQT-----	373
11	A0JJX7	A0JJX7_ASPNG	339	TLYADFSHDNGIISILFALGLYNGTK-PLSTTTVE-----NITQT-----	377
12	Q2XQSO	Q2XQSO_ASPNG	335	TLYADFSHDNGIISILFALGLYNGTK-PLSSTTAE-----NITQT-----	373
13	Q6GYA8	Q6GYA8_ASPNG	335	TLYADFSHDNGIISILFALGLYNGTK-PLSSTTAE-----NITQT-----	373
14	Q9UUZ7	Q9UUZ7_ASPNG	354	TLYADFSHDNGIISILFALGLYNGTK-PLSTTTVQ-----NITQT-----	392
15	O93838	O93838_ASPNG	354	TLYADFSHDNGIISILFALGLYNGTK-PLSSTTAE-----NITQT-----	392
16	Q6T9Z6	Q6T9Z6_ASPNG	354	TLYADFSHDNGIISILFALGLYNGTK-PLSTTTVE-----NITQT-----	392
17	Q6R519	Q6R519_ASPNG	354	TLYADFSHDNGIISILFALGLYNGTK-PLSTTTAE-----NITQT-----	392
18	A2TEY4	A2TEY4_ASPNG	354	TLYADFSHDNGIISILFALGLYNGTK-PLSTTTVE-----NITQT-----	392
19	Q5XNQ8	Q5XNQ8_ASPNG	354	TLYADFSHDNGIISILFALGLYNGTK-PLSTTTVQ-----NITQT-----	392
20	F4ZNF9	F4ZNF9_ASPNG	381	TLYADFSHDNGIISILFALGLYNGTK-PLSSTTAE-----NITQT-----	419
21	A2Q182	A2Q182_ASPNC	329	PLFFNFN-----ISPIITALGIATPAT-PLNKR-----IPFP-----	361
22	A2R685	A2R685_ASPNC	399	SLYDFDAHDYILLGVLTAFGLRQFADLPFPDYTDQYF-MDVFPFR-----	443
23	E3UHI1	E3UHI1_ASPNG	335	TLYADFSHDNGIISILFALGLYNGTK-PLSTTTVE-----NITQT-----	373
24	E3UHI4	E3UHI4_ASPNG	335	TLYADFSHDNGIISILFALGLYNGTK-PLSSTTAE-----NITQT-----	373
25	E3UHI3	E3UHI3_ASPNG	335	TLYADFSHDNGIISILFALGLYNGTK-PLSTTTVQ-----NITQT-----	373
26	E3UHI2	E3UHI2_ASPNG	335	TLYADFSHDNGIISILFALGLYNGTK-PLSSTTAE-----NITQT-----	373
27	E3UHI6	E3UHI6_ASPNG	335	TLYADFSHDNGIISILFALGLYNGTK-PLSSTTAE-----NITQT-----	373
28	E3UHI5	E3UHI5_ASPNG	335	TLYADFSHDNGIISILFALGLYNGTK-PLSTTTVE-----NITQT-----	373
29	E9M258	E9M258_ASPNG	335	TLYADFSHE-----	343
30	Q2MKJ5	Q2MKJ5_ASPNG	338	TLYADFSHDNGIISILFALGLYNGTK-PLSSTTAE-----NITQT-----	376
31	E3UHI7	E3UHI7_ASPNG	335	TLYADFSHDNGIISILFALGLYNGTK-PLSTTTVE-----NITQT-----	373
32	A2R765	A2R765_ASPNC	429	AEYCSF-LDYNVPGQLAKFGLHNGGEQDRWLLNEKWESLALVPVMPDTESSG-GNGEKD	486
33	G3Y5L5	G3Y5L5_ASPNA	421	AEYCPF-LDYNVPGQLAKFGLHNGGEQDEWLLNEKWESLALVPVMPDTESSSTNSGGEKE	479
				;	
				*	

FIGURE 2: Multiple alignment (Clustal O) among the 33 phytases reported for *A. niger*. The green boxes indicate the two phytases reviewed and the red boxes indicate the amino acids that are highly conserved in the active site. The letters shaded in green correspond to positively charged amino acids.

sequence. When the glycation potential analysis was done by using the methodology proposed by Sáenz et al., 2016, the results suggest the glycation of 14 lysines. For Lys₂₁₇, there is no prediction of glycation by either method. Table 4 shows the comparison of the results and distances of the ϵ -NH₂ groups of the lysines and acidic or basic residue side chains. Figure 6 shows some distances between lysines and other acidic or basic residues in 3-phytase B.

3.9. Profile of Antigenicity of 3-Phytase A and Chain A of 3-Phytase B from *A. niger*. The antigenic propensity or average epitope of 3-phytase A is 1.0304; when the average for the complete protein is greater than 1.0 then all residues having more than 1.0 are potentially antigenic. Figure 7(1A) shows the peaks of antigenicity in green colored circles along the chain of amino acids in 3-phytase A. In Figure 7(1B), the two peaks of antigenicity are located on the surface of the protein with higher score in green color and, additionally, its active center in red color is observed, corresponding to the information registered on the antigenic determinants in Table 5. The amino acid Arg₅₈ forms part of the active site of the protein and at the same time is located in an area with a high antigenic propensity, highlighted in underlined font. The letters N highlighted in bold in Table 5 correspond to the positions of the Asparagines (N) which were identified as potential N-glycosylation sites and are also part of some identified antigenic determinant. This finding may be a

contributing factor to the induction of an immune response by 3-phytase A.

The antigenic propensity or average epitope of chain A of 3-phytase B is 1.0234. In Figure 7(2A), the peaks of antigenicity in green circles are observed, along the chain of amino acids in chain A of 3-phytase B. In Figure 7(2B), the peaks of antigenicity in green color are located on the surface of the protein and additionally its active center is observed in red color, corresponding with the information registered on the antigenic determinants in Table 5; the amino acid Arg₁₅₆ is a part of the active site of the protein and, at the same time, is located in an area with a low antigenic propensity, highlighted in underlined font. The letters N highlighted in bold in Table 6 correspond to the positions of the Asparagines (N) which were identified as potential N-glycosylation sites and are also part of some identified antigenic determinant. This finding may be a factor contributing to the induction of an immune response by 3-phytase B.

3.10. Ligand and Molecular Coupling Models (Rigid Docking). The 3D structure of the phytic acid ligand (myo-inositol 1, 2, 3, 4, 5, 6 hexakisphosphate) was generated by the Spartan 4.0 program and is observed in Figure 8. This ligand was used in the molecular coupling models

Molecular coupling models (Rigid Docking) were performed with the two revised phytases from *A. niger* and phytic acid as ligand which was directed to the catalytic

TABLE 1: Physicochemical properties of the two reported and revised phytases from *A. niger*.

Physical and chemical properties (ProtParam)	3-Phytase A (monomer) PDB ID: 3K4Q	3-Phytase B (chain A, Homodimer) PDB ID: IQFX
aa sequence length	467	479
Signal peptide length	23	19
Mature protein length	444	460
Molecular Weight (kDa)	48,84	58,78
Instability Index	45,41 (Unstable)	33,66 (Stable)
Disulfide bond	5 (Intrachain) in positions: Cys ₈ -Cys ₁₇ Cys ₄₈ -Cys ₃₉₁ Cys ₁₉₂ -Cys ₄₄₂ Cys ₂₄₁ -Cys ₂₅₉ Cys ₄₁₃ -Cys ₄₂₁ 4,94	5 (Intrachain) in positions: Cys ₃₂ -Cys ₃₆₈ Cys ₁₀₉ -Cys ₄₅₃ Cys ₁₉₇ -Cys ₄₂₂ Cys ₂₀₆ -Cys ₂₇₉ Cys ₃₉₄ -Cys ₄₀₂ 4,6
Theoretical Isoelectric Point (iP)	4,4 hours (Reticulocytes of mammals, <i>in vitro</i>) >20 hours (yeasts, <i>in vivo</i>) >10 hours (<i>E. coli</i> , <i>in vivo</i>) 72,25 -0,304	1,1 hours (Reticulocytes of mammals, <i>in vitro</i>) 3 minutes (yeasts, <i>in vivo</i>) 2 minutes (<i>E. coli</i> , <i>in vivo</i>) 70,46 -0,33
Estimated Lifetime		
Aliphatic Index		
Average Hydrophobicity (GRAVY)	Ala (A) 29 6.5% Arg (R) 19 4.3% Asn (N) 19 4.3% Asp (D) 29 6.5% Cys (C) 10 2.3% Gln (Q) 19 4.3% Glu (E) 22 5.0% Gly (G) 30 6.8% His (H) 9 2.0% Ile (I) 18 4.1% Leu (L) 36 8.1% Lys (K) 15 3.4% Met (M) 4 0.9% Phe (F) 25 5.6% Pro (P) 22 5.0% Ser (S) 49 11.0% Thr (T) 39 8.8% Trp (W) 4 0.9% Tyr (Y) 18 4.1% Val (V) 28 6.3% Pyl (O) 0 0% Sec (U) 0 0%	Ala (A) 40 8.7% Arg (R) 14 3.0% Asn (N) 38 8.3% Asp (D) 24 5.2% Cys (C) 10 2.2% Gln (Q) 14 3.0% Glu (E) 24 5.2% Gly (G) 37 8.0% His (H) 6 1.3% Ile (I) 19 4.1% Leu (L) 36 7.8% Lys (K) 13 2.8% Met (M) 7 1.5% Phe (F) 20 4.3% Pro (P) 27 5.9% Ser (S) 34 7.4% Thr (T) 32 7.0% Trp (W) 6 1.3% Tyr (Y) 35 7.6% Val (V) 24 5.2% Pyl (O) 0 0% Sec (U) 0 0%
Amino acids composition		
Total number (%) of negatively charged amino acids (Asp + Glu)	51 (11.48%)	48 (10.43%)
Total number (%) of positively charged amino acids (Asp + Glu)	34 (7.65%)	27 (5.86%)

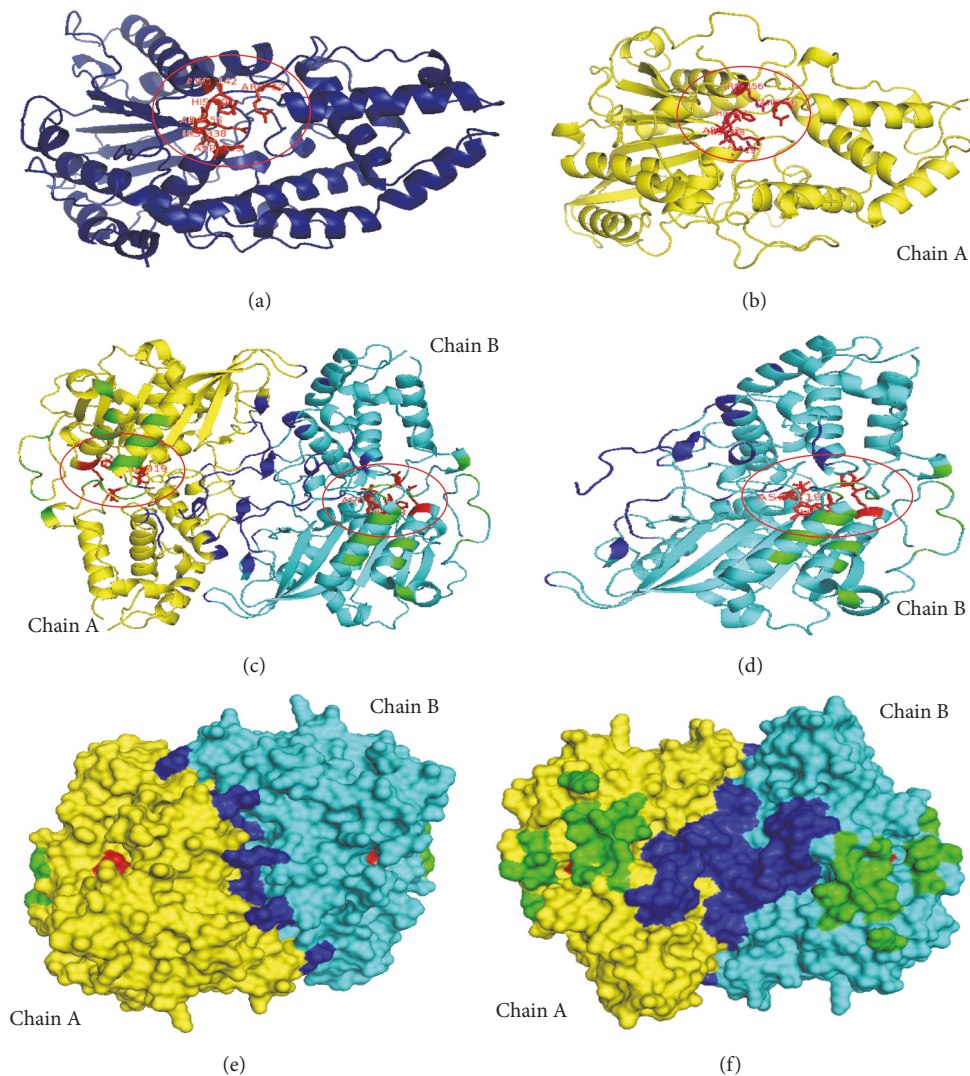


FIGURE 3: (a) *Ribbon diagram of 3-phytase A (PDB ID: 3K4Q)*. The 6 residues marked in red color form part of the pocket of the highly conserved ligand binding active site (R₅₈, H₅₉, G, X(R₆₂), R₁₄₂, X, P, H₃₃₈, D₃₃₉); (b) *ribbon diagram of the 3-phytase B chain A (PDBID: 1QFX)*; the 6 residues indicated in red color form part of the pocket of the highly conserved ligand binding active site (R₆₂, H₆₃, G, X(R₆₆), R₁₅₆, X, P, H₃₁₈, and D₃₁₉); (c) and (d) *active site rear view of the amino acids involved in the interactions that allow dimerization (king blue color), tetramerization (green color), and active ligand binding sites (red color) in the dimer (left) and in the B chain of the 3-phytase B dimer (right)*; (e) *surface diagram of the 3-phytase B top view*; (f) *surface diagram of the 3-phytase B bottom view*.

TABLE 2: Hydrophobicity score in the two reported and revised phytases from *A. niger* (ProtScale). Minimum and maximum values of accessibility in the two reported and revised phytases of *A. niger* (ProtScale).

Physicochemical property	3-Phytase A (444 residues)		3-Phytase B (460 residues)	
	Residue position	Score	Residue position	Score
Hydrophobicity	Ala ₁₆₄	-2.300 (min.)	Glu ₆₅	-2.633 (min.)
	Asp ₆₆	-2.289	Ala ₁₃₅	-2.200
	Ser ₃₁₄	-2.211	Thr ₂₀₄	-2.211
	Ile ₃₄₅	2.722 (max.)	Leu ₃₂₉	3.089 (max.)
	Leu ₃₄₆	2.722 (max.)		
Accessibility	Residue position	Value	Residue position	Value
	Glu ₃₈₇	3.633 (min.)	Gln ₅₆	4.089 (min.)
	Ser ₁₈₂	7.811	Ser ₃₇₄	7.344
	Gly ₆₉	8.467 (max.)	Ser ₇₁	7.389 (max.)

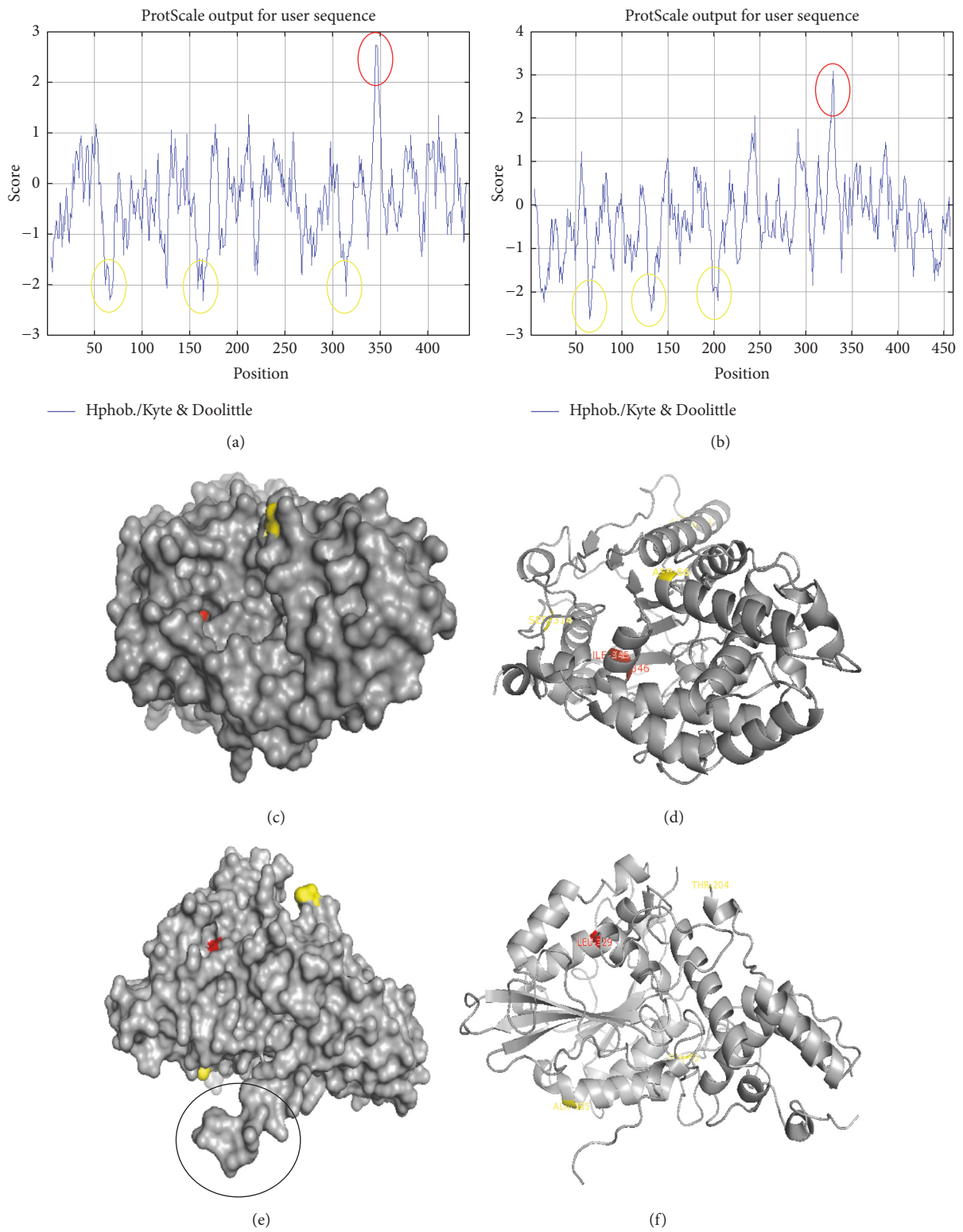


FIGURE 4: *Hydrophobicity profiles* (a and b) of phytases A and B from *A. niger*; (c) and (d) surface and ribbons diagram of the 3-phytase A; (e) and (f) surface and ribbons diagram of the chain A in the 3-phytase B, with the highest scoring amino acids (red color) and lower score (yellow color) of hydrophobicity. The circle in black color refers to the amino acids that allow homodimer formation in the 3-phytase B.

TABLE 3: Possible *N*-glycosylation sites. Three phytases A and B from *A. niger*.

aa position	Potential	Jury agreement	N-Glyc	
<i>Prediction of N-glycosylation sites for 3-phytase A (PDB ID: 3K4Q)</i>				
(1)	27 NQSS	0.5302	(6/9)	+
(2)	59 NESV	0.6564	(9/9)	++
(3)	105 NATT	0.6414	(7/9)	+
(4)	120 NYSL	0.7272	(9/9)	++
(5)	207 NNTL	0.5930	(7/9)	+
(6)	230 NFTA	0.6720	(8/9)	+
(7)	339 NHTL	0.4021	(7/9)	-
(8)	352 NSTL	0.7211	(9/9)	++
(9)	376 NGTK	0.7904	(9/9)	+++
(10)	388 NITQ	0.6418	(8/9)	+
<i>Prediction of N-glycosylation sites for Chain A of 3-phytase B (PDB ID: 1QFX)</i>				
(1)	87 NTTE	0.4822	(4/9)	-
(2)	172 NYST	0.6708	(8/9)	+
(3)	208 NLTY	0.7573	(9/9)	+++
(4)	231 NLTA	0.6870	(9/9)	++
(5)	296 NASL	0.5727	(6/9)	+
(6)	321 NITP	0.1572	(9/9)	---
(7)	406 NYTS	0.6257	(8/9)	+
(8)	423 NVSA	0.5649	(5/9)	+
(9)	439 NTTT	0.5323	(7/9)	+

pocket of the enzymes where the active site (RHGXRP-HD) is located. Figure 9 shows the result of the lower energy docking (-6.3 kcal/mol) between 3-phytase A and phytic acid. Figure 10 provides an overview of the protein and the ligand coupling at the active site.

In Table 6, the results of the five lower docking energies (kcal/mol) obtained with the Autodock program at a distance of 0.375 Å are registered; the amino acids in bold refer to those that make up the highly conserved active site in the histidine acid phosphatases (HAP) and that are involved in the formation of hydrogen bonds with the ligand. In Figure 11, the results recorded in Table 6 are shown. The green dots in Figure 11 refer to the electrostatic interactions involving the formation of hydrogen bonds between the amino acids of the active site and/or the nearest ones to it, and the oxygens or hydrogens of the phytic acid ligand.

Figure 12 shows the docking result between the A chain of the 3-phytase B homodimer and the phytic acid. In Table 6, the results of the first five docking energies (kcal/mol) obtained with the Autodock program are shown. Figure 13 provides an overview of the protein and the ligand coupling at the active site.

In Table 5, the results of the five lower docking energies (kcal/mol) obtained with the Autodock program at a distance of 0.375 Å are recorded; the amino acids in bold refer to those that make up the highly conserved active site in the histidine acid phosphatases (HAP) and that are involved in the formation of hydrogen bonds with the ligand. In Figure 12, the results recorded in Table 2 are evidenced. The green

colored spots in Figure 11 refer to the electrostatic interactions involving the formation of hydrogen bonds between the amino acids of the active site and/or the closest ones to it and the oxygens or hydrogens of the phytic acid ligand.

4. Discussion

The database UNIPROT is characterized for being a nonredundant database, in which, on September 13, 2015, a large number of phytases was reported, 12651 in total, covering different species of microorganisms, plants, and animals. According to Casey and Walsh (2004), 115 (0.9%) phytases belonged to the *Aspergillus* genus, of which 33 (28.69%) corresponded to the species *A. niger*; they asserted that the genus *Aspergillus* is one of the most prolific extracellular producers of phytase enzymes [7].

Of these 33 reported phytases, 11 (33.3%) were found as revised for the genus *Aspergillus*, (phytases that were manually cured by experts in the UNIPROT database). Within this genus, the species *A. terreus* was the one that obtained a greater report of phytases, three in total. However, the three reports for this species corresponded to the same enzyme, 3-phytase A, expressed by the same *phyA* gene. In contrast, the *A. niger* species presented two reports of revised phytases, corresponding to different phytases, the 3-phytase A and the 3-phytase B, expressed by different *phyA* and *phyB* genes, respectively. Both revised phytases from *A. niger* were experimentally obtained by X-ray diffraction [21, 22].

Phytases A2R765 and G3Y5L5 in Figure 1 (green box) were removed from the computational analysis because they

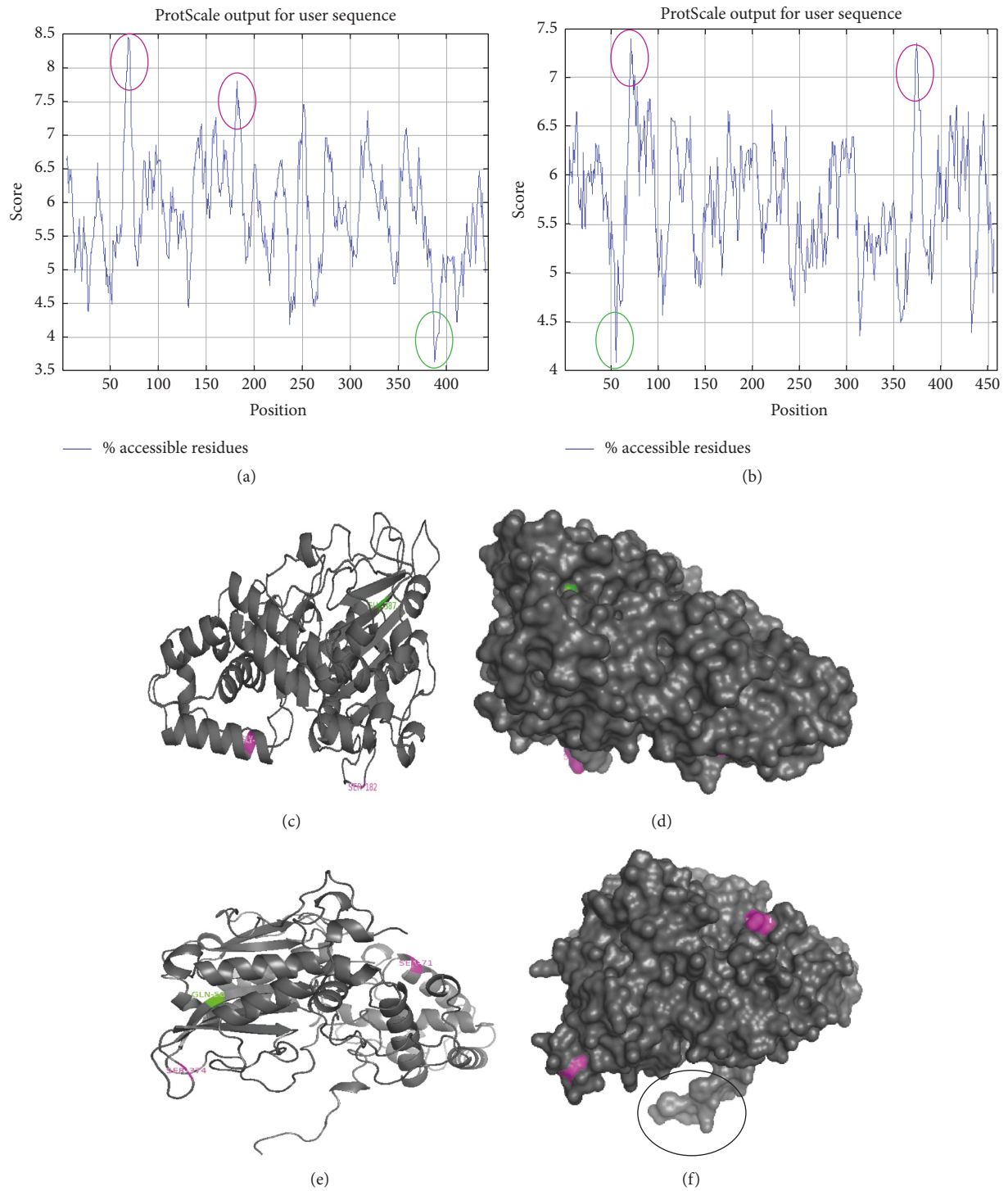


FIGURE 5: Accessibility profiles (a and b) of phytases A and B from *A. niger*. (c) and (d) Surface and ribbons diagram of the 3-phytase A. (e) and (f) Surface and ribbons diagram of chain A in 3-phytase B, where the amino acids with the minimum value (green color) and maximum value (purple) of accessibility are observed. The black colored circle refers to the amino acids that allow homodimer formation in 3-phytase B.

do not have PDB code or are not characterized within UNIPROT.

The ClustalW alignment showed that the sequences of these two phytases reviewed, the 3-phytase A with PDB ID:

3K4Q and the 3-phytase B with PDB ID: 1QFX, are different, being from different proteins. However, the sequences of the chains A and B that form the dimer of 3-phytase B are identical (homodimer). The first revised phytase of A.

TABLE 4: Distances between lysines and acidic or basic residues in the 3D structure of 3-phytase A and the chain A of 3-phytase B and their relation with the prediction of possible glycation sites.

Lysine position	Acid residue distance: Å	Basic residue distance: Å	Glycation prediction Netglycate 1.0 [16] [17]	
<i>3-Phytase A (ID: 3K4Q)</i>				
68	Lys ₆₈ -Glu ₂₀₅ : 8.26	Lys ₆₈ -Lys ₇₀ : 6.51	X	X
70	Lys ₇₀ -Asp ₆₆ : 4.09	Lys ₇₀ -Lys ₇₁ : 9.05; Lys ₇₀ -Lys ₆₈ : 6.51		X
71	Lys ₇₁ -Glu ₂₃₃ : 9.89		X	X
89	Lys ₈₉ -Asp ₂₂₃ : 5.68		X	X
94	Acid residue location > 13.98	Basic residues location > 13.06	—	—
119	Lys ₁₁₉ -Asp ₄₀₅ : 4.21; Lys ₁₁₉ -Asp ₁₂ : 4.27			X
148		Lys ₁₄₈ -Lys ₁₄₉ : 9.73		X
149	Lys ₁₄₉ -Glu ₁₅₂ : 4.52		X	X
158	Lys ₁₅₈ -Asp ₁₆₁ : 7.65		X	X
160	Lys ₁₆₀ -Asp ₁₆₁ : 9.97		X	X
172	Lys ₁₇₂ -Asp ₁₇₄ : 4.50		X	X
254	Lys ₂₅₄ -Asp ₂₄₄ : 9.84			X
277	Lys ₂₇₇ -Asp ₂₃₉ : 7.30; Lys ₂₇₇ -Asp ₂₀₂ : 9.16; Lys ₂₇₇ -Glu ₂₀₅ : 4.28	Lys ₂₇₇ -Lys ₆₈ : 7.84; Lys ₂₇₇ -Lys ₂₇₈ : 6.72		X
278		Lys ₂₇₈ -Lys ₂₇₇ : 6.72; Lys ₂₇₈ -His ₂₈₂ : 6.51		X
356	Lys ₃₅₆ -Asp ₃₇₀ : 8.5; Lys ₃₅₆ -Glu ₃₆₄ : 9.83			X
<i>TOTAL</i>			7	14
<i>Chain A of 3-phytase B (ID: 1QFX)</i>				
14	Lys ₁₄ -Glu ₁₉ : 8.26		X	X
28	Lys ₂₈ -Glu ₃₈ : 8.55; Lys ₂₈ -Asp ₂₂ : 6.95	Lys ₂₈ -His ₂₉ : 8.6		X
61	Lys ₆₁ -Asp ₁₂₅ : 6.56	Lys ₆₁ -His ₃₆₀ : 4.63; Lys ₆₁ -His ₁₂₉ : 4.40		X
74	Lys ₇₄ -Glu ₇₇ : 9.04; Lys ₇₄ -Glu ₇₈ : 4.51; Lys ₇₄ -Asp ₇₅ : 5.95			X
82	Lys ₈₂ -Glu ₇₈ : 9.46; Lys ₈₂ -Asp ₂₃₆ : 4.15			X
92	Lys ₉₂ -Glu ₉₀ : 4.61			X
134		Lys ₁₃₄ -His ₁₃₉ : 9.21		X
163	Lys ₁₆₃ -Glu ₁₅₉ : 8.49; Lys ₁₆₃ -Glu ₁₆₆ : 4.74	Lys ₁₆₃ -Arg ₄₄₇ : 9.84		X
217	Acid residues location > 11.97	Basic residues location > 13.15	—	—
285	Lys ₂₈₅ -Glu ₂₈₄ : 7.35			X
307	Lys ₃₀₇ -Glu ₃₀₈ : 9.81		X	X
413	Acid residues location > 29.31	Basic residues location > 23.84	X	
<i>Total</i>			3	10

niger, the 3-phytase A, corresponds to a monomer and the second phytase revised, the 3-phytase B, corresponds to a homodimer formed by chains A and B. The two revised phytases from *A. niger* also differ in the amount and type of amino acids that form the signal peptide, being 23 residues for 3-phytase A and 19 for 3-phytase B.

The ClustalO alignment (Figure 2) showed that of the 33 reported phytases, 31 (93.9%) share a highly conserved motif corresponding to the active ligand binding site (RHGXRXPHD) in the family of the histidine acid phosphatases “HAP” [22, 24, 25], which allows classification within this family. Within these 31 phytases, 3-phytases A and B (Figure 2, green box), revised phytases for *A. niger* species, were found. Phytases that were not characterized within the UNIPROT database (A2R765 and G3Y5L5), which were not assigned PDB code, did not present this highly conserved motif. Initially, it was possible to detect that the majority of the amino

acids forming this highly conserved active site correspond to positively charged residues (Figure 2, green shading).

The enzymes 3-phytase A and 3-phytase B, belonging to the histidine acid phosphatases family (HAP), have the same enzymatic code E.C.3.1.3.8 according to the database BRENDA, which corresponds to the enzymes with phosphohydrolase activity. These enzymes catalyze the phosphoester bonds of phytic acid, releasing orthophosphate and producing final derivatives such as inositol and inositol monophosphate, which have a lower capacity to bind to metals [25]. This family of phytases share the active site (RHGXRXPHD), whose catalytic pockets are for 3-phytase A (R₅₈, H₅₉, G, X₆₂, R₁₄₂, X, P, H₃₃₈, D₃₃₉) [22] and for the 3-phytase B (R₆₂, H₆₃, G₆₆, X₁₅₆, R₃₁₈, X, P, H₃₁₈, D₃₁₉) [21]; both enzymes have activity at acidic pH (2.5–6.0) and at temperatures between 40 and 60°C, have low substrate specificity, and are capable of hydrolyzing phytate up to inositol monophosphate (IP1), [26].

TABLE 5: Antigenic determinants of 3-phytase A and of chain A in 3-phytase B from *A. niger*.

Fragment number	Position Initial	Sequence	Position Final	Total Number a.a.
<i>Antigenic determinants of 3-phytase A (Long. Total = 444 a.a.)</i>				
<i>Mean antigenic propensity = 1.0304</i>				
1	23	HLWGQYAPFFSLANESVISPEVPAGCRVTEAQVLSR	58	36
2	374	SAWTVPFASRLYVEMMQCAEQEPLRVLVNDRVPLHGCPVDALGR	420	47
<i>Antigenic determinants of chain A in 3-phytase B (Long. Total = 460 a.a.)</i>				
<i>Mean antigenic propensity = 1.0234</i>				
1	322	ITPILAAALGVLPNE	336	15
2	378	TYVRLVLNEAVLPFN	392	15

TABLE 6: Results of lower docking energies between 3-phytase A and the A chain of 3-phytase B versus phytic acid, obtained with the Autodock program.

Classification	Energy (kcal/mol)	Number of hydrogen bonds formed	AA involved
<i>Docking energy between 3-phytase A and phytic acid</i>			
First	-6.3	8	Arg ₅₈ , His ₅₉ , Arg ₆₂ , Arg ₆₂ , Arg ₁₄₂ , Arg ₁₄₂ , His ₃₃₈ , Asp ₃₃₉
Second	-6.2	7	Tyr ₂₈ , Arg ₆₂ , Arg ₆₂ , Arg ₁₄₂ , Arg ₁₄₂ , His ₃₃₈ , Asp ₃₃₉
Third	-6.0	7	Tyr ₂₈ , Arg ₆₂ , Arg ₆₂ , Arg ₆₂ , Lys ₂₇₇ , Lys ₂₇₈ , Asn ₃₄₀
Fourth	-6.0	5	Tyr ₂₈ , His ₅₉ , Arg ₆₂ , Arg ₆₂ , Lys ₂₇₈
Fifth	-5.9	8	Arg ₆₂ , Arg ₁₄₂ , Arg ₁₄₂ , Lys ₂₇₈ , His ₂₈₂ , His ₃₃₈ , Asn ₃₄₀ , Asn ₃₄₀
<i>Docking energy between 3-phytase B chain A and phytic acid</i>			
First	-6.4	3	Arg ₆₂ , Arg ₆₆ , Tyr ₂₇₆
Second	-6.4	4	Arg ₆₆ , Arg ₆₆ , Ser ₆₉ , Ser ₇₁
Third	-6.3	6	Arg ₆₂ , Ser ₇₁ , Try ₁₅₄ , Arg ₁₅₆ , Arg ₁₅₆ , Asn ₂₇₅
Fourth	-6.1	3	Asn ₃₃ , Ser ₆₉ , Tyr ₂₇₆
Fifth	-5.9	4	Asn ₃₃ , Glu ₂₇₂ , Asn ₂₇₅ , Tyr ₂₇₆

The 2D structure of the monomer (Figure 3) of the 3-phytase A and the A chain of the 3-phytase B homodimer (Figure 3) have very similar conformations, being in higher proportion random coils (45% and 50%, resp.) and alpha helices (43% and 38% resp.) in both proteins and in a lower proportion (12% in both proteins) (Figure 3) which provides a more compact structure to both proteins. However, 3-phytase A presents a 3D structure formed by a single domain containing 20 alpha helices and only 8 beta sheets, while the A chain of the homodimer has a more complex structure made up of two domains with the active site located in the interface (Figure 3, red color). The largest domain consists of 11 alpha helices and 8 beta sheets, and the smallest consists of only 10 alpha helices.

The 3-phytase B has two identical A and B chains, which have 39 amino acids (Lys₁₄-Tyr₂₄, Leu₂₇-His₂₉, Tyr₃₆, Glu₃₈, Ser₄₁-Ala₄₅, Tyr₁₂₀, Lys₂₁₇, Leu₂₄₈, Pro₂₅₂-Ser₂₅₄, Gln₂₆₂-Asp₂₆₃, Val₂₆₆-Ser₂₆₇, Asn₃₃₅, Arg₃₄₂, Phe₃₄₅-Gly₃₄₆, Ala₃₇₂, Asp₃₉₃, Gly₃₉₉, Tyr₄₀₀) which allow the interactions that give rise to its dimerization (Figure 3). Kostrewa et al. (1999) obtained a crystal of this protein, formed by a tetramer from two homodimers due to its crystallographic symmetry, and identified 17 amino acids involved in the interactions that facilitate the formation of the tetramer, thus achieving greater stability: Cys₁₀₉, Glu₁₁₄, Thr₁₁₆, Gly₁₁₈, Ala₁₂₁, Leu₁₂₃-Leu₁₂₄,

Tyr₁₂₇-Asn₁₂₈, Asn₁₃₁, Lys₁₆₃, Glu₁₆₆, Tyr₁₇₁, Arg₄₄₇, Pro₄₅₀-Ile₄₅₁, Cys₄₅₃ (Figure 3).

Two N-acetylglucosamine residues, NAG472 and NAG473, from a chain of carbohydrates bound to Asn₁₇₂ are involved in the formation of the homotetramer in the crystal. These carbohydrate chains do not represent the complete natural glycosylation, but result from partial deglycosylation. The main tetramerization contacts are located on the opposite side of the entrance to the active site, so that the four active sites of the tetramer are exposed to the solvent and are easily accessible to the substrate [21].

In Figure 3, the amino acids forming the highly conserved ligand binding site (RHGXRP-HD) in both phytases are detailed, which had initially been determined to be mostly positively charged amino acids (Clustal O alignment), because the ligand "phytic acid" is a very negative organic molecule which, thanks to the presence of the 6 phosphate groups (PO₄⁻³), each of them located in a carbon atom of the inositol ring, binds to this active site by electrostatic interactions of Van der Waals type that generate temporal molecular couplings [27].

The amino acids indicated in red in both phytases correspond to the amino acids that perform the nucleophilic attack, according to the catalytic mechanism proposed by Oh et al. (2004), who assert that the histidine residue in

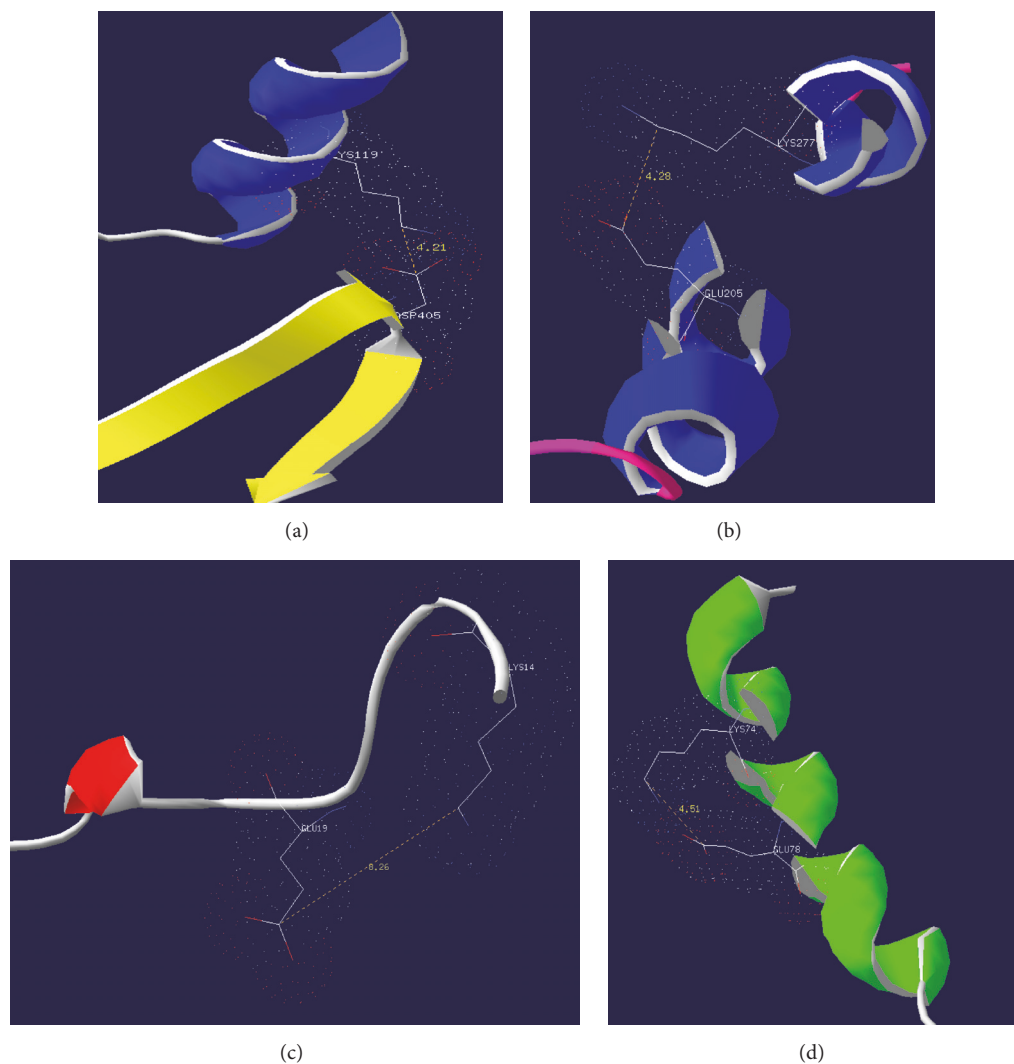


FIGURE 6: Distances between amino acids involved in glycation, Lysine₁₁₉ (a) and Lysine₂₇₇ (b), and acid residues (Asp₄₀₅ and Glu₂₀₅) in the 3D structure of 3-phytase A. Distances between Lysine₁₄ (c) and the Lysine₇₄ (d) and acid residues (Glu₁₉ and Glu₇₈) in the 3D structure of chain A of 3-phytase B.

the highly conserved active site RHGXRXP- serves as a nucleophile in the formation of a covalent phosphohistidine intermediate, while the aspartic acid residue from the C-terminal in the conserved sequence HD serves as a proton donor to the oxygen atom of the cleavable phosphomonoester bond, generating myo-inositol monophosphate as the final product.

The amino acid H₃₃₈ that appears in the legend of Figure 3 between question marks is part of the conserved HD sequence in 3-phytase A that was not reported by Oakley (2010), but that participates in ligand binding; in this research, this amino acid is proposed as a part of the highly conserved active site as observed in molecular docking performed through the Autodock program at a distance of 0.375 Å.

The results obtained by the ProtParam program (Table 1) demonstrated that the 3-phytase A has a length of 444 aa and has a molecular weight of 48.84 kDa. Chain A of 3-phytase B, on the other hand, has a total length of 460 aa in mature state

and a molecular weight of 58.78 kDa. These proteins have a pI of 4.94 and 4.6, respectively, which allows them to be classified as acid phytases.

3-phytase A (monomer) has a higher instability index (45.41) compared to chain A of 3-phytase B, whose instability results are inferior (33.66), which allows to catalog the latest as a stable protein (<40 = stable, values >40 = unstable), possibly due to the fact that the initial formation of the homodimer between the identical chains A and B gives it greater stability. Additionally, the formation of five intrachain disulfide bonds in both chains allows them to stabilize their three-dimensional structure.

The half-life of a protein is a prediction of the time it takes half the concentration of a protein in a cell to degrade after its synthesis. The 3-phytase A, being a monomeric protein, has a longer lifespan (>20 hours in yeast, *in vivo*) possibly because the N-terminal group in its sequence is Alanine (Ala1) and the proteins that possess Met, Ser, Ala, Thr, Val, or Gly at the

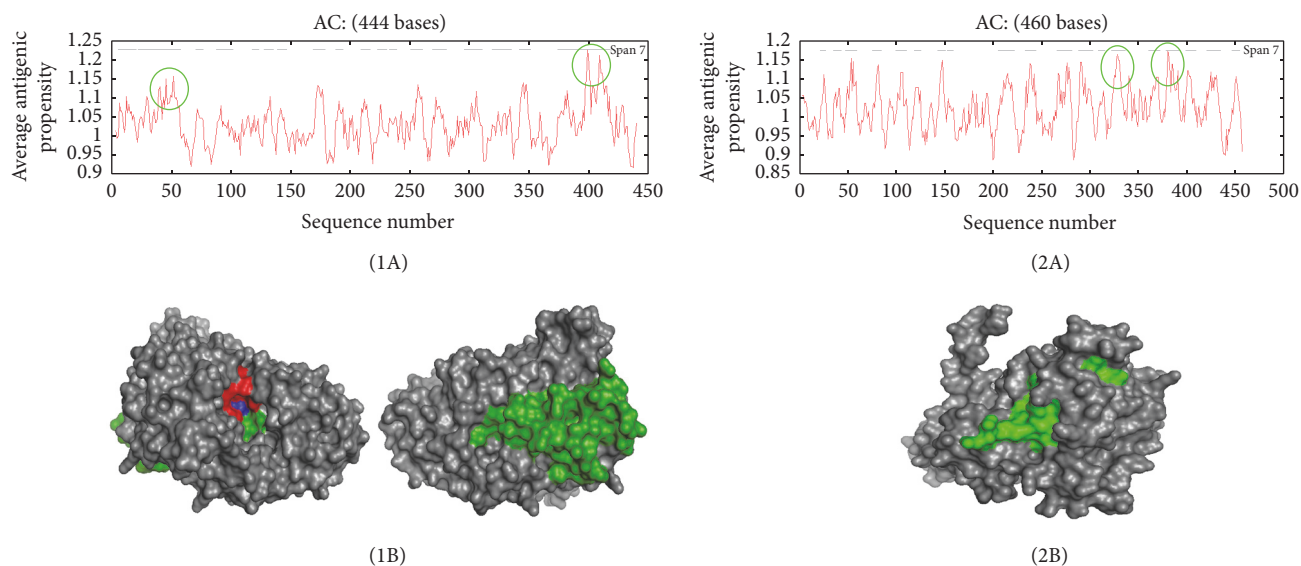


FIGURE 7: *Antigenicity profile.* (1A) 3-Phytase A from *A. niger*; (1B) location of antigenicity peaks (green color). 3-Phytase A from *A. niger* and RHGXRX-HP active site (R_{58} , H_{59} , R_{62} , R_{142} , H_{338} , and D_{339}); (2A) chain A in 3-phytase B from *A. niger*; (2B) location of antigenicity peaks (green color).

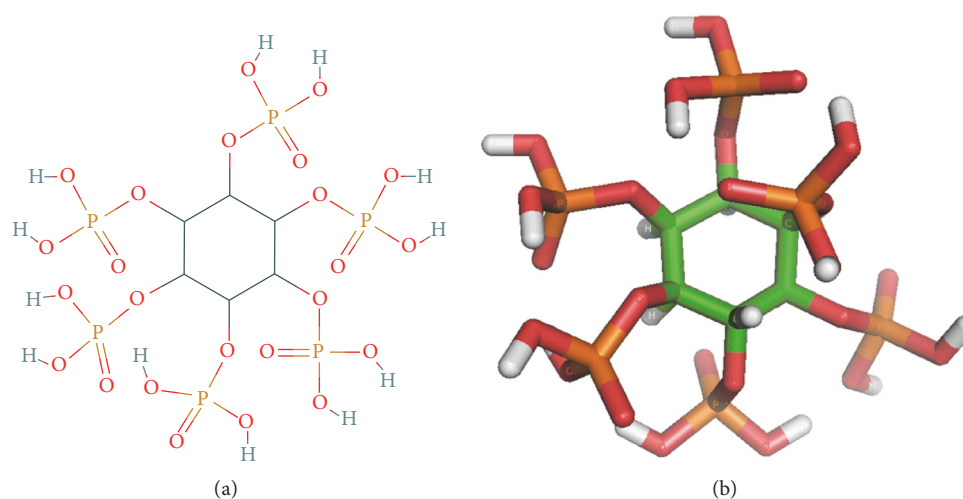


FIGURE 8: *3D structure of phytic acid (myo-inositol 1, 2, 3, 4, 5, 6 hexakisphosphate).* (a) Diagram obtained from Pubchem; (b) 3D model generated by the Spartan 4.0 program and visualized with PyMOL.

N-terminal position register lifespans greater than 20 hours [28, 29].

On the contrary, chain A of 3-phytase B yielded a result of 3 minutes of lifespan in yeast, possibly because the N-terminal group in its sequence is phenyl alanine (Phe_1) and the proteins that have Phe, Leu, Asp, Lys, or Arg at the N-terminal position register lifespans of less than 3 minutes [28, 29]. It appears that this factor involves the ubiquitin system, which is a small protein (76 amino acids) found in all eukaryotic cells and that undergoes an ATP-dependent reaction with proteins, condensing their C-terminal glycine residues with groups of amino of lysines of the protein to

be labeled. These modified proteins are degraded shortly afterwards by a proteolytic complex which is recognized by the ubiquitin marker and because of this their lifespan is very short [28, 29]. The biological importance of the calculation of this parameter lies in the fact that the production of recombinant enzymes takes into account both the lifespan of the proteins to be expressed as well as their stability, in such way that a reduction of the degradation rate of proteins from heterologous genes is achieved.

The results of the aliphatic index of the two revised phytases from *A. niger*, 3-phytase A and 3-phytase B (72.25 and 70.46, resp.), allow the consideration of the fact that the

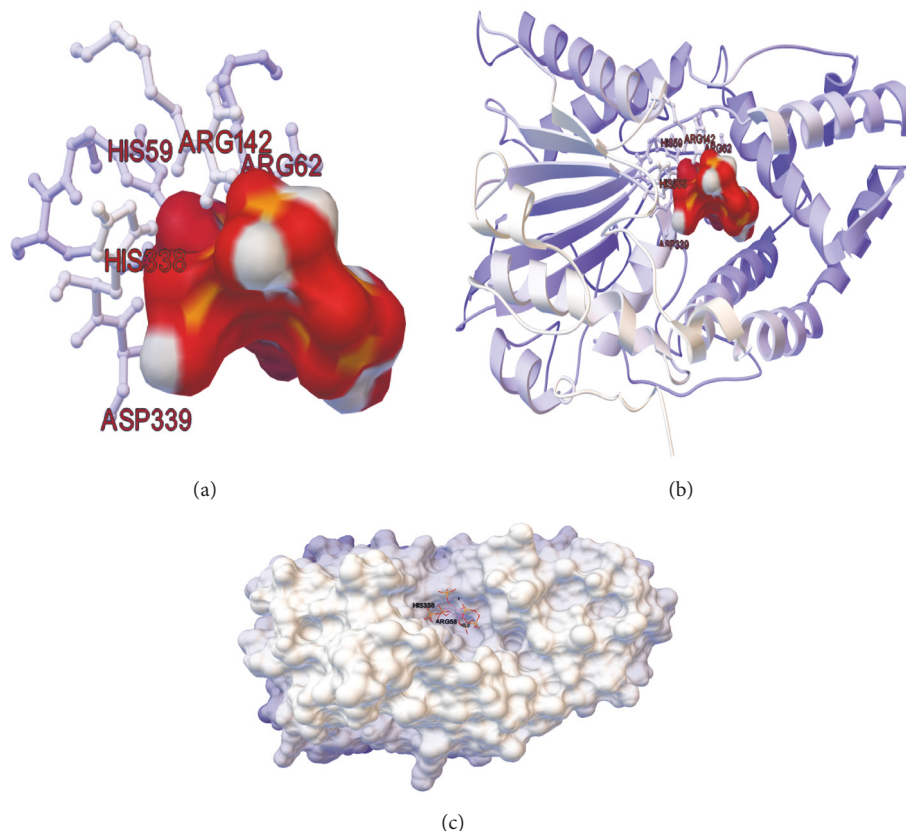


FIGURE 9: Docking result between 3-phytase A (monomer) and phytic acid. (a) Active site (RHGXRX-PHD) consisting of residues R₅₈, H₅₉, R₆₂, R₁₄₂, H₃₃₈, and D₃₃₉ versus phytic acid. (b) Ribbons diagram of the amino acids that make up the active site of the protein and (c) surface diagram of the phytic acid ligand attached to the pocket of the active site of the protein, visualized with the program Autodock.

relative volume occupied by its aliphatic side chains Ala, Val, Ile, and Leu increases thermostability in both phytases (both are globular secretory proteins).

The results of GRAVY (grand average of hydropathy) in 3-phytase A and 3-phytase B (−0.304 and −0.33, resp.) are obtained by combining the values of hydrophobicity and hydrophilicity of the side chains in their sequences. These negative values explain the reason why they tend to interact with aqueous media, typical of secretory proteins such as extracellular phytases [27].

The hydrophobicity profile allowed identifying that amino acids with a high score (Ile₃₄₅ y Leu₃₄₆ in 3-phytase A and Leu₃₂₉ in 3-phytase B, Table 2) were found in areas with little exposure (inside alpha helices, Figures 4(c)–4(f)) in both proteins because such amino acids have aliphatic side chains that do not interact easily with aqueous solvents. On the contrary, amino acids with a minimum hydrophobicity score were found in exposed areas of the proteins (Ala₁₆₄ in 3-phytase A and Glu₆₅ in 3-phytase B). In the case of Glu₆₅, being an amino acid whose R group does not have positive or negative charges at physiological pH, that is, pH close to 6.5 and 7.0, allows it to be solubilized more easily in aqueous solvents and, in the case of Ala₁₆₄, to have a short aliphatic side chain that allows it to interact more easily with the aqueous medium. It should be noted that none of these

amino acids were a part of the active site of ligand binding in both phytases. The amino acids indicated within the black circle in Figure 4(e) are involved in the formation of the homodimer in 3-phytase B and therefore are not found within an exposed zone of the protein. In general terms, 3-phytase A and 3-phytase B present few hydrophobic regions, as expected in secretory proteins [27].

The accessibility profile allowed the identification of the amino acids more or less exposed to the solvent, according to the score obtained and recorded in Table 2. For the 3-phytase A and the 3-phytase B, the Gly₆₉ and the Ser₇₁, respectively, were located in areas that were very exposed to the solvent and that were not a part of the active ligand binding site (Figures 5(c)–5(f)). The amino acid glycine has a simple structure, is the smallest amino acid, and is the only nonchiral amino acid, characteristics that allow it to acquire special conformations that other amino acids can not, and for this reason obtains a high solvent accessibility score. As for the serine amino acid, although it has an uncharged R polar group (−OH), it is short, very reactive, and hydrophilic, with a tendency to form hydrogen bonds with water.

The amino acids with the lowest accessibility score (Glu₃₈₇ in 3-phytase A and Gln₅₆ in 3-phytase B) were located inside the protein as a part of beta sheets (Figures 5(c)–5(f)) because glutamine is a polar amino acid and glutamic acid

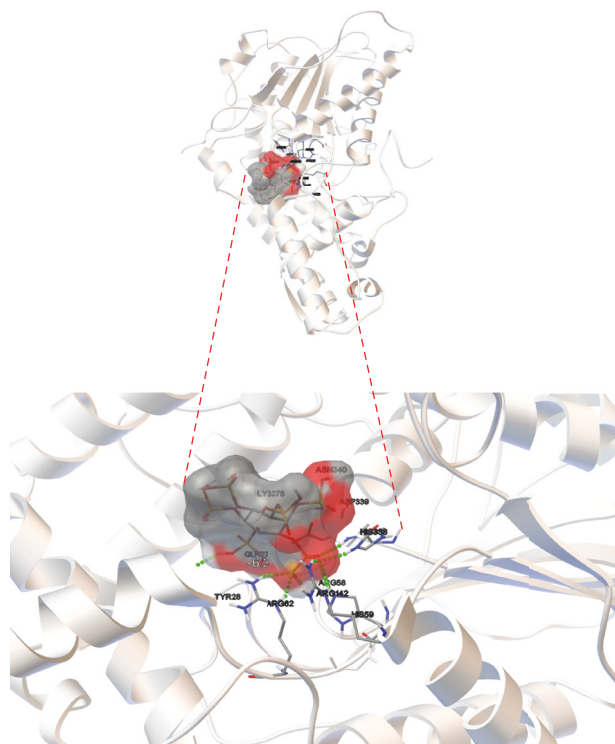


FIGURE 10: General overview of the docking result between 3-phytase A and phytic acid (lowest energy = -6.3 kcal/mol). Active site (RHGXRX-P-HD) consisting of residues R₅₈, H₅₉, R₆₂, R₁₄₂, H₃₃₈, and D₃₃₉ versus phytic acid, visualized with the Autodock program. The red colored areas in the phytic acid correspond to regions with negative charge. Green dots refer to the H Bridges established between the ligand and the amino acids that form the active site in the protein.

is negatively charged, which reduces its exposure to the solvent. According to the hydrophobicity profile, 3-phytase A and 3-phytase B present a high proportion of zones of easy accessibility to the aqueous medium along their sequences.

Secretory proteins, such as phytase enzymes, have carbohydrate addition or glycosylation sites that allow them to be recognized in the rough endoplasmic reticulum for their future correct folding and secretion [30, 31]. Using the NetNGlyc 1.0 bioinformatics program, 9 N-glycosylation sites for 3-phytase A (monomer) and 7 N-glycosylation sites for 3-phytase B (dimer) chain A were established. The positions of the Asparagines (N) along both phytase chains that were located in an Asn-Xaa-Ser/Thr section (where Xaa is any amino acid except proline) could be glycosylated (Table 3). It stands out that the seven possible N-glycosylation sites predicted for chain A of 3-phytase B must be duplicated because this phytase is formed by two identical chains, A and B, that initially form a homodimer; for that reason, it would have a total of 14 possible N-glycosylation sites for this phytase. The carbohydrate that binds directly to these N-glycosylation sites is normally N-acetylglucosamine [21, 22]. These added sugars will promote the correct folding of the phytases, deducing a mechanism of quality control of

synthesis and assembly of the proteins, thus increasing its stability [32].

In glycation, the initial reversible reaction occurs between aldehyde or ketone groups of reducing sugars and ϵ -NH₂ groups of lysines or the amino terminal of the protein. Subsequently, there is formation of Amadori products and finally AGEs (*Advanced Glycation End products*) are formed [33]. In general, the amino groups with the lowest pKa value should be more reactive towards glycation due to their nucleophilic capacity [34]. In the case of lysines, it has been suggested that the proximity of nearby residues plays a determining role to be or not glycated. The positively charged amino acids located near the primary structure or the three-dimensional structure decrease the pKa and thereby catalyze the glycation of such lysines [35]. Likewise, it has been suggested that the proximity of an acid residue to a lysine catalyzes the formation of Amadori products, which would make lysine more reactive to be glycated [36]. The results of the comparison of lysine prediction by the Netglycate algorithm [16], which exclusively considers the primary sequence of the protein and the methodology proposed by Sáenz et al. (2016), which uses the 3D structure of the protein, are shown in Table 4 and allow us to point out that, for the case of 3-phytase A, according to the proposal of the spatial relationship between the ϵ -NH₂ group and side chains of acidic or basic residues as a requirement for glycation, 14 lysines with distances inferior to 9.89 Å are considered as potentially glycable. Although these distances exist in the 3D structure, only seven were considered by the algorithm Netglycate 1.0. The only lysine without glycation prediction by the two methodologies presented distances above 13.06 Å between the ϵ -NH₂ group and the side chains of basic or acidic residues, a distance that would not allow the chemical interaction between these chemical groups as a requirement for glycation.

For the case of chain A of 3-phytase B, of the 10 lysines susceptible to being glycated as proposed by Sáenz et al. (2016), all with distances lower than 9.48 Å, only two are considered by Netglycate 1.0. The third lysine with prediction of glycation (K₄₁₃) is not considered by this proposal since the group ϵ -NH₂ is separated from the side chains of basic or acidic residues by distances greater than 23.84 Å, a distance that would not allow the chemical interaction between these chemical groups as a requirement for glycation. The only lysine not considered by the two methodologies is K₂₁₇, whose ϵ -NH₂ group is located away from the side chains of basic or acidic residues by distances greater than 13.15 or 11.97 Å, respectively, distances that would not allow the chemical interaction between these chemical groups as a requirement for glycation.

Ninety percent (9/10) of the Netglycate 1.0 predictions, as proposed by Sáenz et al. (2016), can be associated with the spatial relationship between lysines and acidic or basic residues less than 10 Å and the remaining 10% (1/10), the K₄₁₃ of IQFX, presents distances greater than 23.84 Å to acidic or basic residues even though, according to the data provided by the algorithm Netglycate 1.0, its probability (score) of occurrence of glycation is scarcely 59.8% (data not

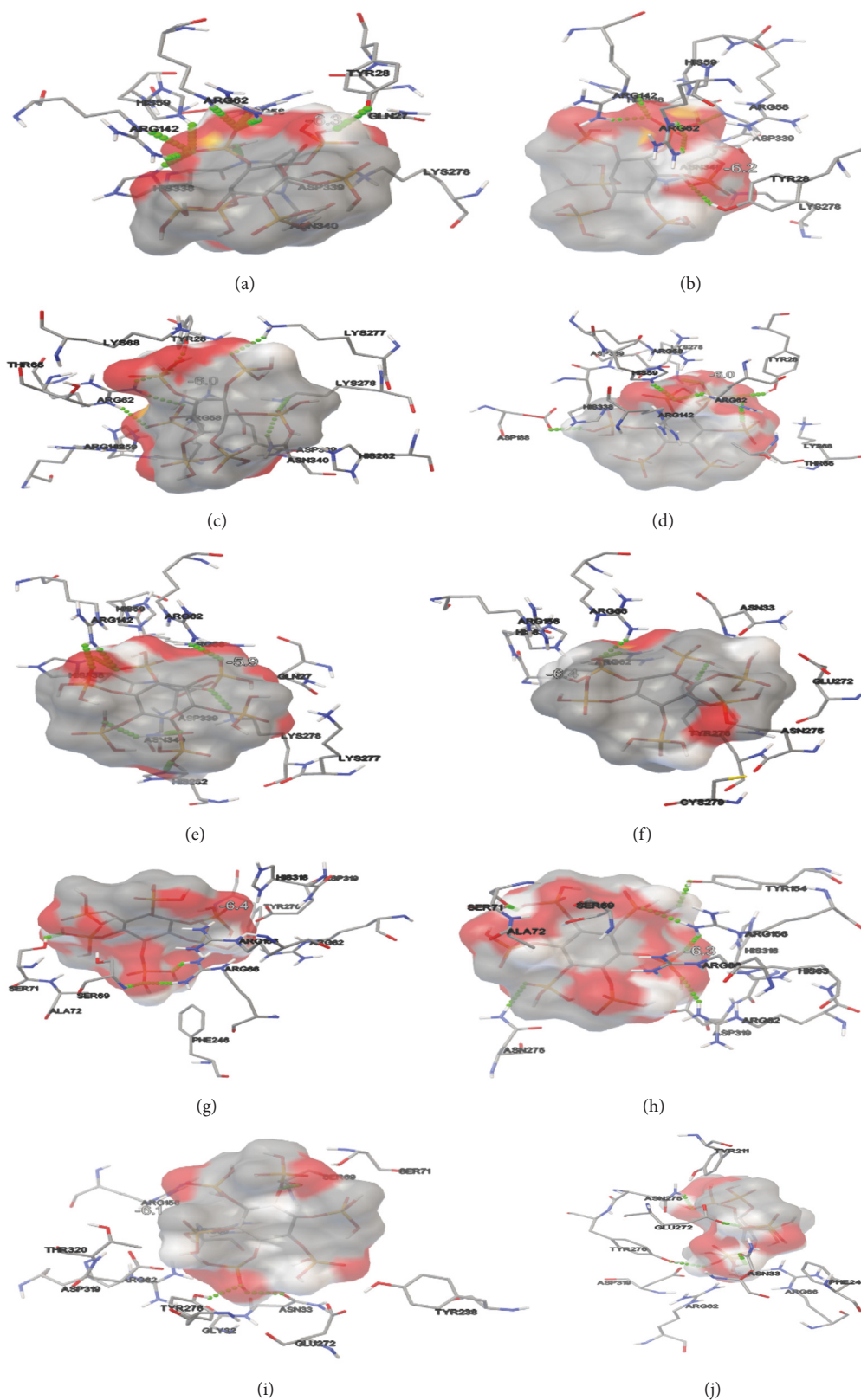


FIGURE 11: Van der Waals electrostatic interactions involving the formation of hydrogen bonds (green dots) between the active site amino acids and/or those closest to it in 3-phytase A (a–e), chain A of 3-phytase B (f–j), and the oxygens or hydrogens of the phytic acid ligand. Red colored regions can be seen, corresponding to negative regions in the electrostatic cloud of the ligand that make contact with the amino acids of the protein.

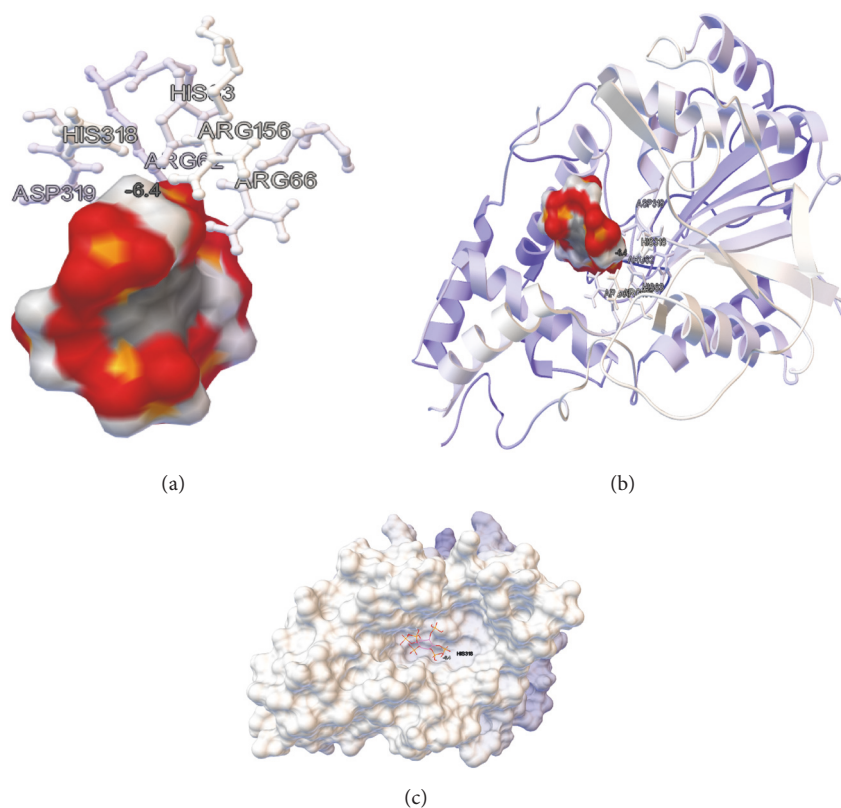


FIGURE 12: Result of the docking between the A Chain of the homodimer from 3-phytase B and the phytic acid. (a) Active site (RHGXRX-P-HD) consisting of residues R₆₂, H₆₃, R₆₆, R₁₅₆, H₃₁₈, and D₃₁₉ versus phytic acid. (b) Ribbons diagram of the amino acids that compose the active site of the protein and (c) surface diagram of the phytic acid ligand attached to the pocket of the active site of the protein, visualized with the program Autodock.

shown), being the lowest of all; however, it is predicted to be potentially glyicable.

These results are in accordance with what Sáenz et al. (2016) proposed, because it is not necessarily the sequence (primary structure) but the spatial relationship in the 3D structure that favors the lysines glycation, provided that the distances of lysines to acidic or basic residues are less than 10 Å (Figure 6). In this sense, this type of enzymes with high percentages of acidic and basic residues and lysines close, in both the primary structure and the 3D structure, to acid residues or other basic residues generates a high probability of chemical interaction between that type of amino acids, required for glycation. Finally, the Netglycate algorithm only predicted as glyicable lysines 37.5% of those proposed by Sáenz et al. (2016).

“*In vitro*” investigations with other proteins that have been brought into contact with reducing sugars show that glycation may affect biological activity [37]. Assays performed with recombinant human interferon-gamma (hIFN- γ) glycoprotein isolates in *E. coli* demonstrated that such purified protein was also prone to progressive proteolysis and covalent dimerization during storage, since late glycation stages cause the cleavage of the peptide bond and the covalent reticulation in lysine and arginine residues (but not of cysteine) [38]; that is to say that glycation promotes protein fragmentation

and is produced in glycated lysines [17]. However, the “*in vitro*” effect caused in proteins should be studied carefully to correctly determine the cause-effect relationship, since the observed phenomena could be the consequence of the glycation of other components that can interact with the proteins or of the reactions between the protein and some by-product generated during glycation [37]. Therefore, the identification of these potential glycation sites in 3-phytase A and 3-phytase B chain A could represent potential sites of fragmentation of the concentrated or purified proteins during prolonged storage times, negatively affecting their biological activity.

In 3-phytase A, the average antigenic propensity was 1.0304, and when the average value is higher than 1.0, the amino acids that are above 1.0 will be potentially antigenic. According to the data recorded in Table 5 and compared to Figure 7(1A) (Green colored circles), two highly antigenic peaks or regions can be identified. The first region groups the amino acids from His₂₃-Arg₅₈, 36 amino acids in total including the amino acid Arg₅₈, which is the first amino acid that forms part of the ligand binding active site and is therefore part of a solvent accessible zone. The second region registers the highest peak of antigenicity and integrates a greater amount of amino acids from Ser₃₇₄-Arg₄₂₀, 47 amino acids in total, being located in the opposite side to the active

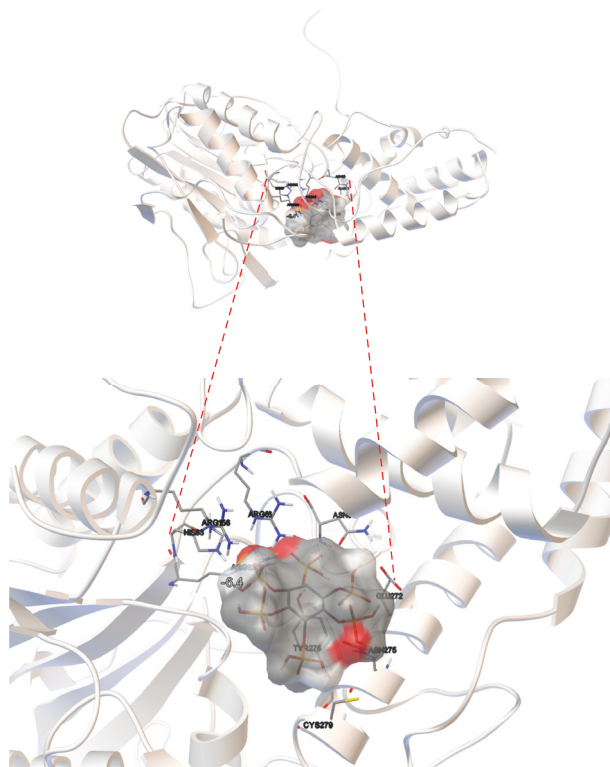


FIGURE 13: General overview of the docking result between the A chain of the 3-phytase B homodimer and the phytic acid (lowest energy = -6.4 kcal/mol). Active site (RHGXRX-HD) consisting of residues R₆₂, H₆₃, R₆₆, R₁₅₆, H₃₁₈, and D₃₁₉ versus phytic acid, visualized with the Autodock program. The red colored areas in the phytic acid correspond to regions with negative charge.

site and in a zone highly exposed to the solvent, as can be observed in Figure 7(1B). The prediction of antigenic peptides takes into account which peptide fragments of a protein are likely to be antigenic. These antigenic fragments should be located in solvent accessible regions and should contain hydrophobic and hydrophilic residues. Therefore, the second region which comprises the highest amount of amino acids and is completely exposed to the solvent would have a higher antigenicity.

In chain A of 3-phytase B, the average antigenic propensity is 1.0234. In contrast to 3-phytase A, the 3-phytase B chain A has more peaks or highly antigenic regions that cluster fewer amino acids; however, according to the data recorded in Table 5 and compared to Figure 7(2A) (green colored circles), two highly antigenic peaks or regions can be identified. The first region groups the amino acids Ile₃₂₂-Glu₃₃₆, 15 amino acids in total, located in an area highly exposed to the solvent. The second region contains amino acids Thr₃₃₈-Asn₃₉₂, 15 amino acids in total, but not all of them are exposed to the solvent. Five of these 15 are hydrophobic (Val₃₈₀, Leu₃₈₂, Val₃₈₃, Leu₃₈₄, and Val₃₈₈) and therefore are located in the interior of the protein (Figure 7(2B)). Therefore, antigenic fragments of the first region, which are all located in solvent accessible regions and contain hydrophobic and hydrophilic residues, would exhibit greater antigenicity.

The positions of the Asparagines (N) that were identified as potential N-glycosylation sites and which are a part of the reported antigenic determinants are highlighted in bold in Table 5 because this is a factor that may contribute to the induction of an immune response by both phytases [39].

Considering the usefulness of phytases as a dietary supplement in monogastric animals, it is also pertinent to consider that the presence of regions with high antigenic propensity along the sequence of these proteins could be translated in the presence of allergens that could trigger an allergic reaction in the host, who ingests them. The process of digestion involves mechanical, chemical, and biochemical processes that allow macronutrients to be transformed into simpler molecules that can be absorbed and used by animals. But despite the fact that these digestive processes take place, significant amounts of protein from diets and that are immunologically active reach the intestinal mucosa of monogastric animals [40]. When there is an actual allergic reaction, the body produces antibodies (proteins that specifically bind to allergens to neutralize and remove them from the body). There are different types of antibodies, but the responsible for allergic reactions to food is known as immunoglobulin E (IgE). The IgE antibody binds to the allergens, triggering an allergic reaction. During this reaction, IgE activates the segregation of signaling molecules in the bloodstream, which simultaneously causes the common symptoms of food

allergies such as skin rashes, inflammation, abdominal pain and inflammation, vomiting, and diarrhea [40]. However, in several investigations performed [41–43] in animals, no reports were found on allergic reactions provoked by phytases to the animals involved in the trials.

In the research conducted by Kostrewa et al. (1999) and Oakley (2010), the ligand used to obtain the crystalline structure of 3-phytase A and 3-phytase B, respectively, was myo-inositol-1,2,3,4,5,6-hexakis sulfate (IHS), a potent inhibitor of such enzymes. This chemical compound is isosteric and isoelectric with respect to myo-inositol 1, 2, 3, 4, 5, 6 hexakisphosphate (IHP) and is considered an excellent analogous substrate.

However, the ligand used in this investigation corresponded to the chemical compound myo-inositol 1, 2, 3, 4, 5, 6 hexakisphosphate (IHP), also called phytic acid, the main form of phosphorus storage in the cereals that make up the diet of monogastric animals. This chemical compound is highly negative due to the presence of 6 phosphate groups (PO_4^{-3}) in its inositol ring, which is why the active site of binding to this ligand in phytases is composed mainly of positively charged amino acids (RHGXRXD), [21, 22].

The molecular coupling model (Rigid Docking) directed to the catalytic pocket of 3-phytase A formed by residues Arg₅₈, His₅₉, Arg₆₂, Arg₁₄₂, His₃₃₈, and Asp₃₃₉ [22], and phytic acid as ligand, yielded very interesting results that allowed establishing the formation of Van der Waals electrostatic interactions that generated hydrogen bonds between the amino acids that form the active site of the protein and the oxygen or hydrogen of the phosphate groups of phytic acid (Figure 11). The lowest 5 energies of the molecular coupling result were selected (Table 6) and it was possible to determine which amino acids were forming the hydrogen bonds.

Table 6 shows that in the case of 3-Phytase B there are 6 amino acids (Arg₅₈, His₅₉, Arg₆₂, Arg₁₄₂, His₃₃₈, and Asp₃₃₉) of the active center involved in the formation of 8 hydrogen bonds with phytic acid, generating the lower energy in docking (−6.3 kcal/mol), which is favorable because the greater number of hydrogen bonds formed between the active site of the enzyme and the ligand favors the stability of this temporary molecular interaction [27].

Research by Oakley (2010) reported that the amino acids that form the active site of the protein and therefore establish electrostatic Van der Waals type interactions with the analogous IHP ligand in the crystal by the X-ray diffraction method at a resolution of 2.20 Å are: Arg₅₈, His₅₉, Arg₆₂, Arg₁₄₂ and Asp₃₃₉. However, the active site of the protein in histidine acid phosphatases presents highly conserved residues (RHGXRXD), involving a histidine in the HD segment. By means of the molecular coupling (Rigid Docking) carried out in this investigation at a distance of 0.375 Å, it was possible to determine that the His₃₃₈ is involved in the formation of a hydrogen bond with the phytic acid ligand that was not previously reported by Oakley (2010), but was consistent with the information reported in the PDBsum database [22].

For the molecular coupling model (Rigid Docking) directed to the catalytic pocket of chain A of 3-phytase B, formed by residues Arg₆₂, His₆₃, Arg₆₆, Arg₁₅₆, His₃₁₈, and

Asp₃₁₉ [21] and phytic acid as ligand, the formation of Van der Waals electrostatic interactions that generated hydrogen bonds between the amino acids that form the active site of the protein and the oxygens or hydrogens from the phosphate groups of phytic acid was also detected (Figure 11). The lowest 5 energies of the molecular coupling result were selected (Table 6) and it was possible to determine which amino acids were forming the hydrogen bonds.

Table 6 shows that in the case of 3-Phytase B there are 6 amino acids (Arg₆₂, Ser₇₁, Try₁₅₄, Arg₁₅₆, Arg₁₅₆, and Asn₂₇₅) of the active center involved in the formation of 4 hydrogen bonds with phytic acid, generating the lower energy in docking (−6.3 kcal/mol).

It is interesting to note that Kostrewa et al., (1999) determined that the active site of 3-phytase B is subdivided into a catalytic center (R₆₂, H₆₃, R₆₆, R₁₅₆, H₃₁₈ y D₃₁₉) and a substrate specificity site (Asp₇₅ and Glu₂₇₂); however, only the amino acid Arg₆₆ forms part of this active site and participates in the formation of the hydrogen bonds with the analogous substrate IHS in the crystal [21].

Table 6 shows the energy of docking number 2 (−6.4 Kcal/mol) which involves 3 of these amino acids (Arg₆₆, Ser₆₉ and Ser₇₁); although they do not form a part of the active center of the protein, they do form hydrogen bonds with the analog substrate IHS in the crystal. In addition, they are reported in PDBsum. Therefore, taking into account the fact that the stability of this temporal molecular interaction depends mainly on the number of hydrogen bonds formed, the energy that would offer greater stability would be number 3, since it additionally involves a greater number of amino acids than those that are located in the active site of the enzyme [27].

5. Conclusions

The species *Aspergillus niger* expresses two phytases currently reported by the UNIPROT database: 3-phytase A (PDB ID: 3K4Q) corresponding to a monomer and 3-phytase B (PDB ID: IQFX) corresponding to a homodimer (chains A and B) which, due to its crystallographic symmetry, generates a homotetramer from two dimers. These phytases have been crystallized and the genes encoding them (*phyA* and *phyB* gene, resp.) have been cloned and overexpressed in other microorganisms, which has allowed them to be widely used in the feed industry of monogastric animals. The computational characterization of the two phytases produced by *A. niger*, 3-phytase A and 3-phytase B, made it possible to establish that both phytases belong to the histidine acid phosphatases class, with the active ligand binding site (RHGXRXD) highly conserved. The 3-phytase A and the 3-phytase B chain A possess a molecular length and a molecular weight that do not differ substantially, although the monomer is considered as an unstable protein and the homodimer has a shorter lifespan. The aliphatic index in both phytases allows to conclude that they are thermostable enzymes. The hydrophobicity profiles and accessibility showed that these phytases interact with aqueous media, which is a characteristic of secretory proteins. It was possible to identify possible glycosylation and glycation sites in both phytases, which could affect the correct folding

of the proteins and their possible fragmentation during prolonged storage times and therefore their biological activity. Both 3-phytases, A and B, exhibited areas with high antigenic propensity which could affect the immune system of the animal that ingests them. Finally, the molecular coupling models in both phytases allowed verifying the formation of electrostatic interactions of Van der Waals type that generates hydrogen bonds between the amino acids that form the active center of the protein and the oxygens or hydrogens of the phosphate groups of phytic acid, providing greater stability to these temporary molecular interactions.

Disclosure

The funders had no role in study design, data collection and analysis, decision to publish, or preparation of the manuscript.

Conflicts of Interest

The authors have declared that no conflicts of interest exist.

Authors' Contributions

Doris C. Niño-Gómez and Claudia M. Rivera-Hoyos contributed equally to this work.

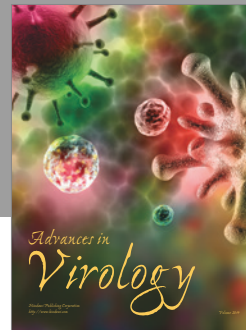
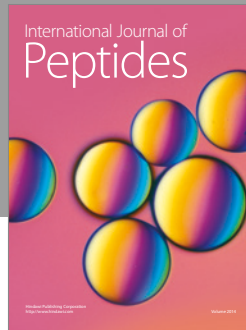
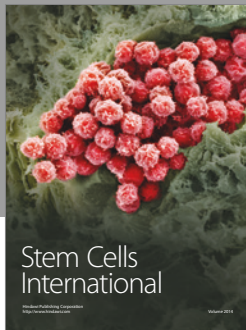
Acknowledgments

This work was supported by Pontificia Universidad Javeriana, Bogotá, Colombia (Grant ID 00007390) titled “Clonación y expresión constitutiva de las Fitasas 3-Fitasa A y 3-Fitasa B de *Aspergillus niger* bajo el control del pGAP en *Pichia pastoris*,” by Universidad Nacional de Colombia, Bogotá, Colombia (Grant DIB 201010020419) and by Universidad Centroccidental Lisandro Alvarado, Barquisimeto, Venezuela (Grant CDCHT ICS-2017-6). The authors thank María Lucía Gutiérrez for English editing.

References

- [1] B. L. Lim, P. Yeung, C. Cheng, and J. E. Hill, “Distribution and diversity of phytate-mineralizing bacteria,” *The ISME Journal*, vol. 1, no. 4, pp. 321–330, 2007.
- [2] A. Acosta and M. Cárdenas, “Enzimas en la alimentación de las aves. Fitasas,” *Revista Cubana de Ciencia Agrícola*, vol. 40, no. 4, pp. 377–387, 2006.
- [3] Y. Zhu, X. Qiu, Q. Ding, M. Duan, and C. Wang, “Combined effects of dietary phytase and organic acid on growth and phosphorus utilization of juvenile yellow catfish *Pelteobagrus fulvidraco*,” *Aquaculture*, vol. 430, pp. 1–8, 2014.
- [4] P. Vats and U. C. Banerjee, “Production studies and catalytic properties of phytases (myo-inositolhexakisphosphate phosphohydrolases): an overview,” *Enzyme and Microbial Technology*, vol. 35, no. 1, pp. 3–14, 2004.
- [5] S. Dahiya and N. Singh, “Isolation and biochemical characterization of a novel phytase producing bacteria *Bacillus cereus* isolate MTCC 10072,” *International Journal of Microbial Resource Technology*, vol. 2, no. 2, pp. 1–5, 2014.
- [6] M. Lamid, N. N. T. Puspaningsih, and O. Asmarani, “Potential of phytase enzymes as biocatalysts for improved nutritional value of rice bran for broiler feed,” *Journal of Applied Environmental and Biological Sciences*, vol. 4, no. 3, pp. 377–380, 2014.
- [7] A. Casey and G. Walsh, “Identification and characterization of a phytase of potential commercial interest,” *Journal of Biotechnology*, vol. 110, no. 3, pp. 313–322, 2004.
- [8] G. E. A. Awad, M. M. I. Helal, E. N. Dania, and M. A. Esawy, “Optimization of phytase production by *Penicillium purpurogenum* GE1 under solid state fermentation by using Box-Behnken design,” *Saudi Journal of Biological Sciences*, vol. 21, no. 1, pp. 81–88, 2014.
- [9] A. Pandey, G. Szakacs, C. R. Soccol, J. A. Rodriguez-Leon, and V. T. Soccol, “Production, purification and properties of microbial phytases,” *Bioresource Technology*, vol. 77, no. 3, pp. 203–214, 2001.
- [10] The UniProt Consortium, “Reorganizing the protein space at the Universal Protein Resource (UniProt),” *Nucleic Acids Research*, vol. 40, no. D1, pp. D71–D75, 2012.
- [11] S. F. Altschul, T. L. Madden, A. A. Schäffer et al., “Gapped BLAST and PSI-BLAST: a new generation of protein database search programs,” *Nucleic Acids Research*, vol. 25, no. 17, pp. 3389–3402, 1997.
- [12] W. Li, A. Cowley, M. Uludag et al., “The EMBL-EBI bioinformatics web and programmatic tools framework,” *Nucleic Acids Research*, vol. 43, no. 1, pp. W580–W584, 2015.
- [13] H. Berman, K. Henrick, and H. Nakamura, “Announcing the worldwide Protein Data Bank,” *Nature Structural Biology*, vol. 10, no. 12, p. 980, 2003.
- [14] E. Gasteiger, C. Hoogland, A. Gattiker et al., *Protein Identification and Analysis Tools on the ExPASy Server*, Humana Press, New York, NY, USA, 2005.
- [15] G.-Y. Chuang, J. C. Boyington, M. Gordon Joyce et al., “Computational prediction of N-linked glycosylation incorporating structural properties and patterns,” *Bioinformatics*, vol. 28, no. 17, Article ID bts426, pp. 2249–2255, 2012.
- [16] M. B. Johansen, L. Kiemer, and S. Brunak, “Analysis and prediction of mammalian protein glycation,” *Glycobiology*, vol. 16, no. 9, pp. 844–853, 2006.
- [17] H. Sáenz-Suárez, R. A. Poutou-Piñales, J. González-Santos et al., “Prediction of glycation sites: new insights from protein structural analysis,” *Turkish Journal of Biology*, vol. 40, no. 1, pp. 12–25, 2016.
- [18] N. Guex and M. C. Peitsch, “SWISS-MODEL and the Swiss-PdbViewer: an environment for comparative protein modeling,” *Electrophoresis*, vol. 18, no. 15, pp. 2714–2723, 1997.
- [19] A. S. Kolaskar and P. C. Tongaonkar, “A semi-empirical method for prediction of antigenic determinants on protein antigens,” *FEBS Letters*, vol. 276, no. 1-2, pp. 172–174, 1990.
- [20] G. M. Morris, H. Ruth, W. Lindstrom et al., “Software news and updates AutoDock4 and AutoDockTools4: automated docking with selective receptor flexibility,” *Journal of Computational Chemistry*, vol. 30, no. 16, pp. 2785–2791, 2009.
- [21] D. Kostrewa, M. Wyss, A. D’Arcy, and A. P. G. M. Van Loon, “Crystal structure of *Aspergillus niger* pH 2.5 acid phosphatase at 2.4 Å resolution,” *Journal of Molecular Biology*, vol. 288, no. 5, pp. 965–974, 1999.
- [22] A. J. Oakley, “The structure of *Aspergillus niger* phytase PhyA in complex with a phytate mimetic,” *Biochemical and Biophysical Research Communications*, vol. 397, no. 4, pp. 745–749, 2010.

- [23] J. Söding, "Protein homology detection by HMM-HMM comparison," *Bioinformatics*, vol. 21, no. 7, pp. 951–960, 2005.
- [24] B.-C. Oh, W.-C. Choi, S. Park, Y.-O. Kim, and T.-K. Oh, "Biochemical properties and substrate specificities of alkaline and histidine acid phytases," *Applied Microbiology and Biotechnology*, vol. 63, no. 4, pp. 362–372, 2004.
- [25] E. J. Mullaney and A. H. J. Ullah, "The term phytase comprises several different classes of enzymes," *Biochemical and Biophysical Research Communications*, vol. 312, no. 1, pp. 179–184, 2003.
- [26] E. Humer, C. Schwarz, and K. Schedle, "Phytate in pig and poultry nutrition," *Journal of Animal Physiology and Animal Nutrition*, vol. 99, no. 4, pp. 605–625, 2015.
- [27] D. L. Nelson and M. M. Cox, *Lehninger, Principles of Biochemistry*, Freeman and Company, New York, NY, USA, 5th edition, 2005.
- [28] M. Hochstrasser, "Ubiquitin, proteasomes, and the regulation of intracellular protein degradation," *Current Opinion in Cell Biology*, vol. 7, no. 2, pp. 215–223, 1995.
- [29] A. Varshavsky, "The N-end rule: functions, mysteries, uses," *Proceedings of the National Academy of Sciences of the United States of America*, vol. 93, no. 22, pp. 12142–12149, 1996.
- [30] A. J. Parodi, "Role of N-oligosaccharide endoplasmic reticulum processing reactions in glycoprotein folding and degradation," *Biochemical Journal*, vol. 348, no. 1, pp. 1–13, 2000.
- [31] A. Helenius and M. Aeby, "Intracellular functions of N-linked glycans," *Science*, vol. 291, no. 5512, pp. 2364–2369, 2001.
- [32] R. S. López, "El proceso de N-glicosilación de proteínas en *Entamoeba histolytica*," *Revista Latinoamericana de Microbiología*, vol. 48, no. 2, pp. 70–72, 2006.
- [33] P. Verbeke, B. F. C. Clark, and S. I. S. Rattan, "Modulating cellular aging in vitro: hormetic effects of repeated mild heat stress on protein oxidation and glycation," *Experimental Gerontology*, vol. 35, no. 6-7, pp. 787–794, 2000.
- [34] H. F. Bunn, R. Shapiro, M. McManus et al., "Structural heterogeneity of human hemoglobin A due to nonenzymatic glycosylation," *Journal of Biological Chemistry*, vol. 254, no. 10, pp. 3892–3898, 1979.
- [35] N. Iberg and R. Fluckiger, "Nonenzymatic glycosylation of albumin *in vivo*. Identification of multiple glycosylated sites," *Journal of Biological Chemistry*, vol. 261, no. 29, pp. 13542–13545, 1986.
- [36] J. W. Baynes, N. G. Watkins, C. I. Fisher et al., "The Amadori product on protein: structure and reactions," *Progress in Clinical and Biological Research*, vol. 304, no. 24, pp. 43–67, 1989.
- [37] F. L. González Flecha, P. R. Castello, J. J. Gagliardino, and J. P. F. C. Rossi, "La glucosilación no enzimática de proteínas. Mecanismo y papel de la reacción en la diabetes y el envejecimiento," *Ciencia al Día Internacional*, vol. 3, no. 2, pp. 1–17, 2000.
- [38] R. Mironova, T. Niwa, R. Dimitrova, M. Boyanova, and I. Ivanov, "Glycation and post-translational processing of human interferon- γ expressed in *Escherichia coli*," *Journal of Biological Chemistry*, vol. 278, no. 51, pp. 51068–51074, 2003.
- [39] M. López-Hoyos, G. Fernández-Fresnedo, H. López-Escribano, and A. de Francisco, "Antigenicidad de las proteínas recombinantes," *Gaceta Médica de Bilbao*, vol. 101, no. 1, pp. 17–21, 2004.
- [40] J. L. C. Muñoz, "Antigenicidad de piensos y materias primas proteicas en conejos," in *Departamento de Ciencia Animal*, p. 120, Universidad Politécnica de València, València, España, 2016.
- [41] Y. B. Wu, V. Ravindran, and W. H. Hendriks, "Effects of microbial phytase, produced by solid-state fermentation, on the performance and nutrient utilisation of broilers fed maize- and wheat-based diets," *British Poultry Science*, vol. 44, no. 5, pp. 710–718, 2003.
- [42] J. P. Zhou, Z. B. Yang, W. R. Yang, X. Y. Wang, S. Z. Jiang, and G. G. Zhang, "Effects of a new recombinant phytase on the performance and mineral utilization of broilers fed phosphorus-deficient diets," *Journal of Applied Poultry Research*, vol. 17, no. 3, pp. 331–339, 2008.
- [43] D. Šefer, B. Petrujkić, R. Marković et al., "Effect of phytase supplementation on growing pigs performance," *Acta Veterinaria*, vol. 62, no. 5-6, pp. 627–639, 2012.



Hindawi

Submit your manuscripts at
<https://www.hindawi.com>

